

AD-A048 229

NORTH TEXAS STATE UNIV DENTON DEPT OF PHYSICS

F/6 20/5

INVESTIGATION OF LASER OPTICAL BIASING ON THE QUANTUM TRANSPORT--ETC(U)

OCT 77 D G SEILER

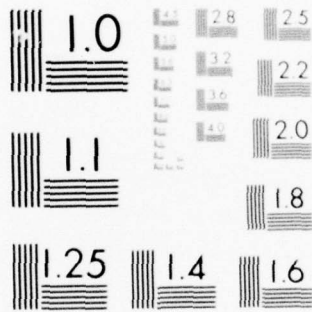
N00014-76-C-0319

UNCLASSIFIED

NL

| OF |
AD
A048229





MICROCOPY RESOLUTION TEST CHART
NATIONAL BUREAU OF STANDARDS-1963-A

ADA048229

12

Annual Summary Report
Investigation of Lung Cancer
Causes of the Disease
The National Cancer Institute

U.S. GOVERNMENT PRINTING OFFICE
1975

REPORT DOCUMENTATION PAGE		READ INSTRUCTIONS BEFORE COMPLETING FORM
1. REPORT NUMBER	2. GOVT ACCESSION NO.	3. RECIPIENT'S CATALOG NUMBER
6. TITLE (and Subtitle) <u>Investigation of</u> <u>LASER OPTICAL BIASING OF THE QUANTUM</u> <u>TRANSPORT PROPERTIES OF n-InSb.</u>		9. TYPE OF REPORT & PERIOD COVERED <u>Annual summary rept.</u> <u>1 Oct 1976 - 30 Sept 1977</u>
7. AUTHOR(s) <u>DAVID G. SEILER</u>		15. CONTRACT OR GRANT NUMBER(s) <u>N00014-76-C-0319</u>
8. PERFORMING ORGANIZATION NAME AND ADDRESS <u>DEPARTMENT OF PHYSICS</u> <u>NORTH TEXAS STATE UNIVERSITY</u> <u>DENTON, TEXAS 76203</u>		10. PROGRAM ELEMENT, PROJECT, TASK AREA & WORK UNIT NUMBERS
11. CONTROLLING OFFICE NAME AND ADDRESS <u>ONR Electronic and Solid State Sciences Program</u> <u>Office of Naval Research</u> <u>Arlington, VA 22217</u>		12. REPORT DATE <u>Oct 1977</u>
14. MONITORING AGENCY NAME & ADDRESS (if different from Controlling Office) <u>ONR Resident Representative</u> <u>528 Federal Building</u> <u>300 East 8th Street</u> <u>Austin, Texas 78701</u>		13. NUMBER OF PAGES <u>65</u> <u>12/72 p.</u>
16. DISTRIBUTION STATEMENT (of this Report)		18. SECURITY CLASS. (of this report) <u>Unclassified</u>
17. DISTRIBUTION STATEMENT (of the abstract entered in Block 20, if different from Report)		
19. SUPPLEMENTARY NOTES		
18. KEY WORDS (Continue on reverse side if necessary and identify by block number) <u>InSb</u> <u>Quantum Transport</u> <u>Optical Biasing</u> <u>Photoexcited carriers</u>		
20. ABSTRACT (Continue on reverse side if necessary and identify by block number) <u>CO₂ laser induced hot electrons in n-InSb have been studied at liquid helium</u> <u>temperatures by determining the effect of the laser radiation on the amplitude</u> <u>of Shubnikov-de Haas oscillations. Phenomenological values for the electron</u> <u>temperature and the energy relaxation time of the electron gas are determined</u> <u>for a sample of 1.5 x 10¹⁵ cm⁻³ concentration.</u> <u>A new technique for investigating hot electron oscillatory magnetoresistance</u> <u>has been utilized in obtaining fundamental information concerning the effects</u> <u>of CO₂ laser radiation and high electric fields on the quantum transport (Cont.)</u>		

DD FORM 1 JAN 73 1473

EDITION OF 1 NOV 65 IS OBSOLETE
S/N 0102-014-6601

20. properties of n-InSb.

FOREWORD

This Annual Summary Report by David G. Seiler, Department of Physics, North Texas State University covers research progress for the period October 1, 1976 to September 30, 1977.

ACCESSION FOR	
HYTS	Wing Section <input checked="" type="checkbox"/>
DOC	Buff Section <input type="checkbox"/>
UNANNOUNCED	<input type="checkbox"/>
JUSTIFICATION	
<i>Letter on file</i>	
BY	
DISTRIBUTION/AVAILABILITY CODES	
Dist.	AVAIL. AND OR SPECIAL
A	

SUMMARY

Experiments have shown that CO_2 laser-induced changes in the Shubnikov-de Haas (SdH) effect in n-InSb provide a new tool for studying the properties of the laser-induced hot electrons. During the time the sample is illuminated the SdH amplitudes are found to decrease with increasing laser power in a manner analogous to the effect of increasing lattice temperature. Consequently, these results give direct evidence for a CO_2 laser-induced increase in the electron energy of InSb and permit the extraction of electron temperatures. A phenomenological value for the energy relaxation time can also be derived using a simple energy balance approach. Using an estimated value for the power absorbed per electron, energy relaxation times of about 25 nsec are determined.

A new experimental technique was conceived and subsequently discovered to improve the sensitivity of measuring the hot electron magnetophonon effect in InSb under application of high electric fields. This technique is completely adaptable to any oscillatory magnetoresistance measurement and has thus proven extremely valuable in the laser-induced hot electron studies. The capabilities of this new technique were investigated by studying the extremely high resolution data obtainable on the electric-field induced hot-electron magnetophonon effect in n-InSb. Both amplitudes and extremal positions as a function of electric fields were studied in the transverse

and longitudinal configurations.

Investigation of ohmic (low electric field) magnetophonon structure has produced several new results. Magnetophonon structure has been observed for the first time in a degenerate sample of n-InSb of concentration $7.5 \times 10^{15} \text{ cm}^{-3}$ at 77 K. The positions of the resistance maxima appear at higher magnetic fields than those found in pure ($\leq 10^{14} \text{ cm}^{-3}$) samples. The nonparabolicity of the InSb conduction band has been shown to play a role even in the pure samples. In the higher doped samples, there is an increasing contribution of higher order transitions.

In summary, much progress has been made during this year as documented in this report.

TABLE OF CONTENTS

I.	FOREWORD	i
II.	SUMMARY	ii
III.	TABLE OF CONTENTS	iv
IV.	EXPERIMENTAL WORK	1
	A. Lasers	1
	1. cw CO	1
	2. cw CO ₂	9
	B. Development of a Magnetic Field Modulation Technique for the Measurement of Oscillatory Magnetoresistance Phenomena Using Short Voltage Pulses	13
V.	EXPERIMENTAL RESULTS	18
	A. Magnetophonon Studies	18
	1. Low Electric Field Region	18
	2. High Electric Field Region	22
	B. Laser Induced Changes in the Shubnikov-de Haas Effect	24
	1. Pulsed dc Method	24
	2. Magnetic Field Modulation Method	26
VI.	FUTURE PLANS	41
	A. Experimental	41
	1. Lasers	41
	2. Installation of Electro-Optic Switch	41

3.	Extension of CO ₂ Laser-Induced Hot Electron Measurements to Higher Carrier Concentrations . .	42
4.	Measurements of CO Laser-Induced Hot Electrons . .	42
B.	Theoretical	43
VII.	TECHNICAL PERSONNEL	46
VIII.	REPORT ON INTERNATIONAL CONFERENCE ON HOT ELECTRONS, JULY 6-8, 1977, HELD AT NTSU, DENTON, TEXAS	47
IX.	SUMMARY OF PRINCIPLE ACCOMPLISHMENTS DURING OCTOBER 1, 1976 THROUGH SEPTEMBER 30, 1977	64

IV. EXPERIMENTAL WORK

A. Lasers

1. cw CO

The continuous wave carbon monoxide laser has been the subject of many theoretical and experimental studies.¹⁻⁶ Due to the nature of the pumping mechanism and discharge kinetics, the CO laser is extremely sensitive to impurities such as O_2 , H_2O , H_2 , and hydrocarbons. To eliminate these contaminants from the laser discharge tube and provide a high purity environment for the laser gas mixture, a high vacuum system has been constructed as shown in Figure 1. This system utilizes an oil diffusion pump with a liquid nitrogen cold trap to produce a clean vacuum. An ionization gauge is incorporated to measure the high vacuum region. Other vacuum gauges include thermocouple tubes to monitor backing and roughing pressures and a Wallace and Tiernan gauge to measure the laser gas fill pressure. An optic-dense metallic foreline trap is used on the roughing line to eliminate backstreaming of pump oil into the system.

For successful high power operation the temperature of the gas must be lowered. To achieve this a recirculating alcohol cooling system has been built. As shown in Figure 2, this cooling system uses a closed cycle in which ethyl alcohol is passed through a heat transfer coil immersed in an alcohol bath contained within an insulated tank. This alcohol bath is cooled by dry ice or liquid nitrogen. Stable operation using dry ice has been achieved at $-68^\circ C$ (205K). The temperature of the recirculating alcohol and the alcohol

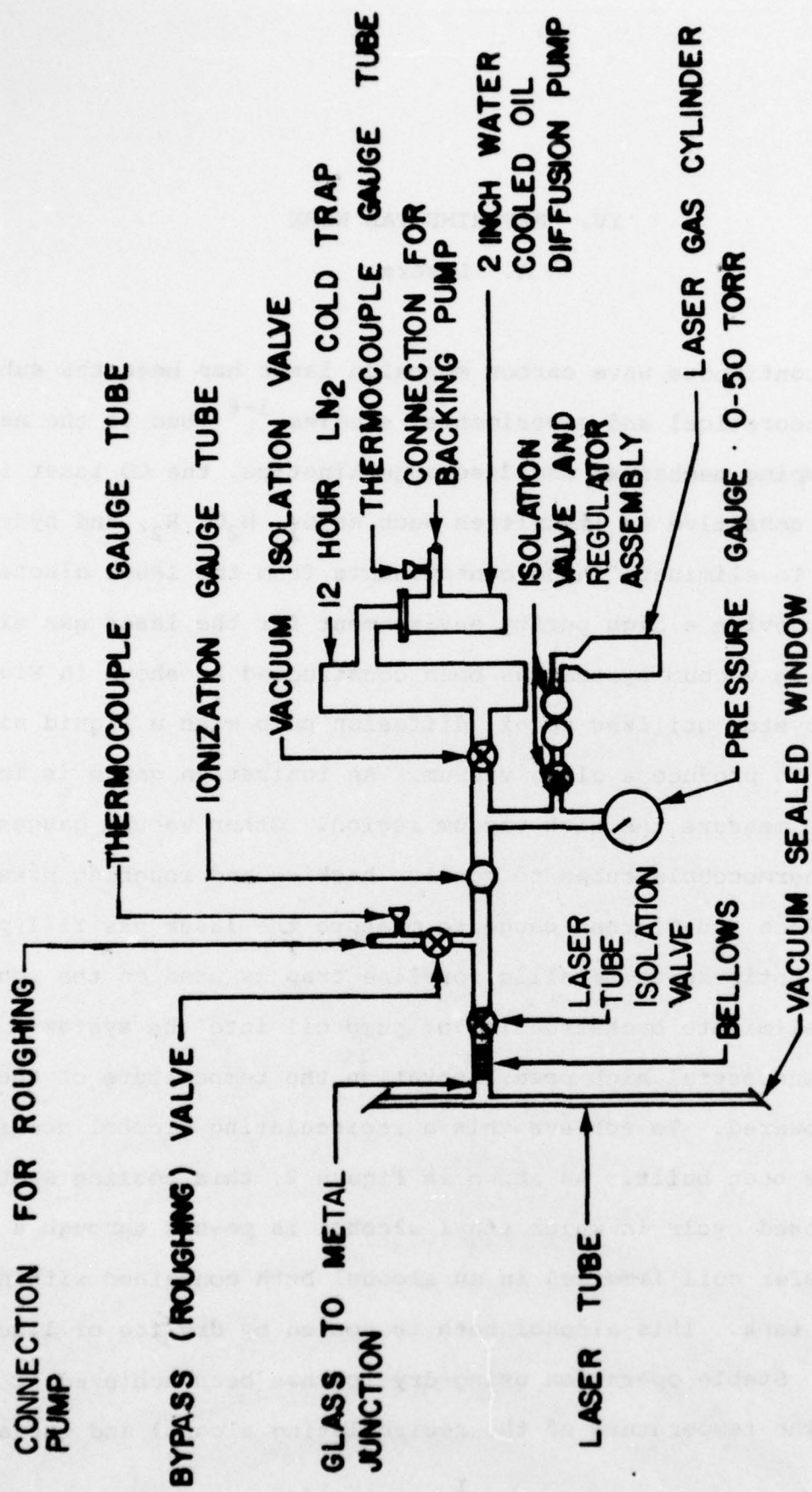


Figure 1. CO LASER VACUUM SYSTEM

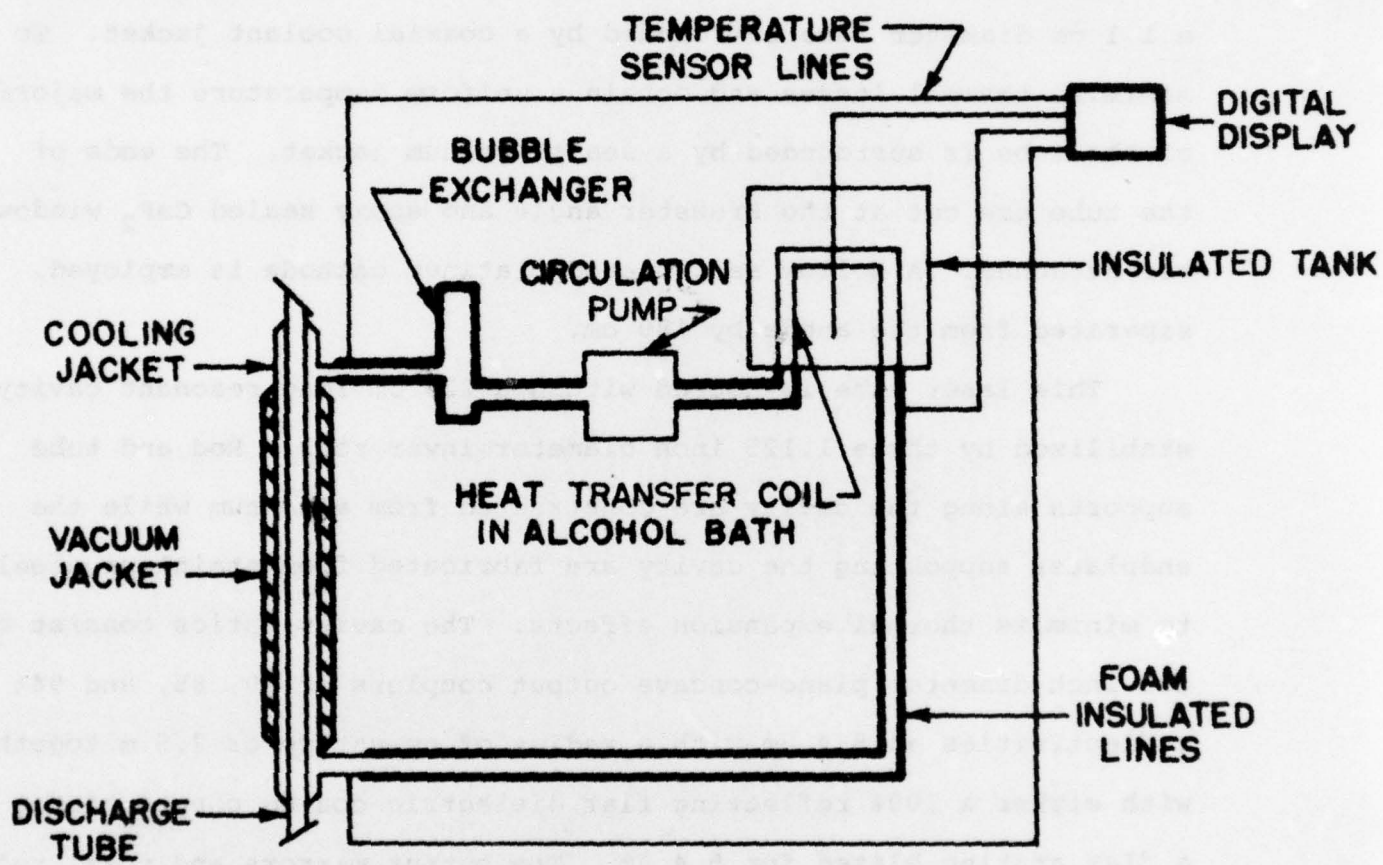


Figure 2. CO LASER COOLING SYSTEM

bath is monitored at several points by copper-constantan thermocouples using a liquid nitrogen reference junction and a digital millivoltmeter readout.

The laser tube itself consists of a triple wall pyrex structure shown in Figure 3. The overall length of the tube is 2 cm with a maximum outer diameter of 4.5 cm. The discharge region is a 1.1 cm diameter tube surrounded by a coaxial coolant jacket. To minimize thermal losses and obtain a uniform temperature the majority of the tube is surrounded by a sealed vacuum jacket. The ends of the tube are cut at the Brewster angle and epoxy sealed CaF_2 windows are attached. A hollow self heated platinum cathode is employed, separated from the anode by 180 cm.

This laser tube is housed within a 220 cm long resonant cavity stabilized by three 1.125 inch diameter invar rods. Rod and tube supports along the cavity are constructed from aluminum while the endplates supporting the cavity are fabricated from stainless steel to minimize thermal expansion effects. The cavity optics consist of one inch diameter plano-concave output couplers of 70, 85, and 94% reflectivities at $5.4 \mu\text{m}$ with a radius of curvature of 7.5 m together with either a 100% reflecting flat dielectric coated copper mirror or a flat grating blazed for $5.4 \mu\text{m}$. The output mirrors and total reflector are held in micrometer driven high resolution optical mounts. The grating is contained in a mount with a micrometer drive to provide rotation for wavelength selection. Adjustable irises are employed on each end of the cavity for mode restriction.

The laser gas is a mixture of 6.06%, 6.28% N_2 , 6.30% Xe and the balance is He. A stainless steel Linde Ultra Pure regulator

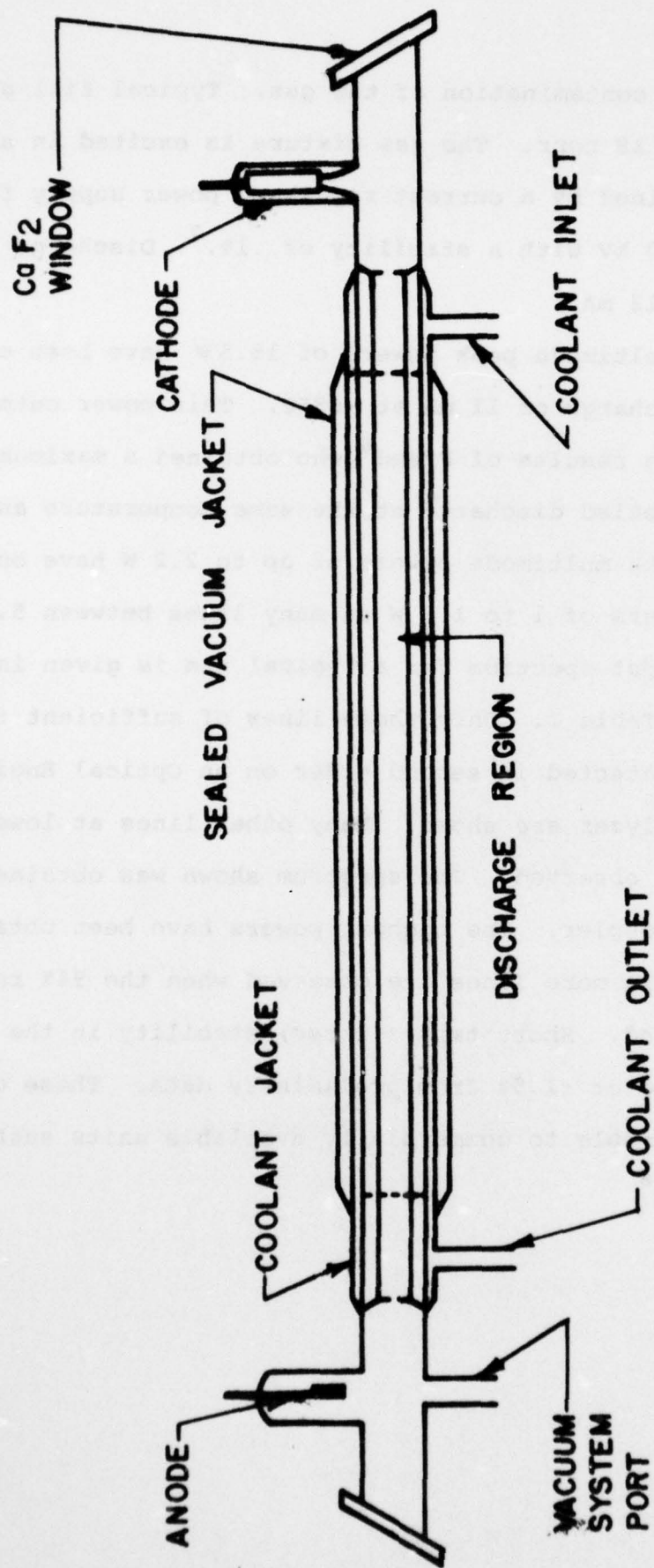
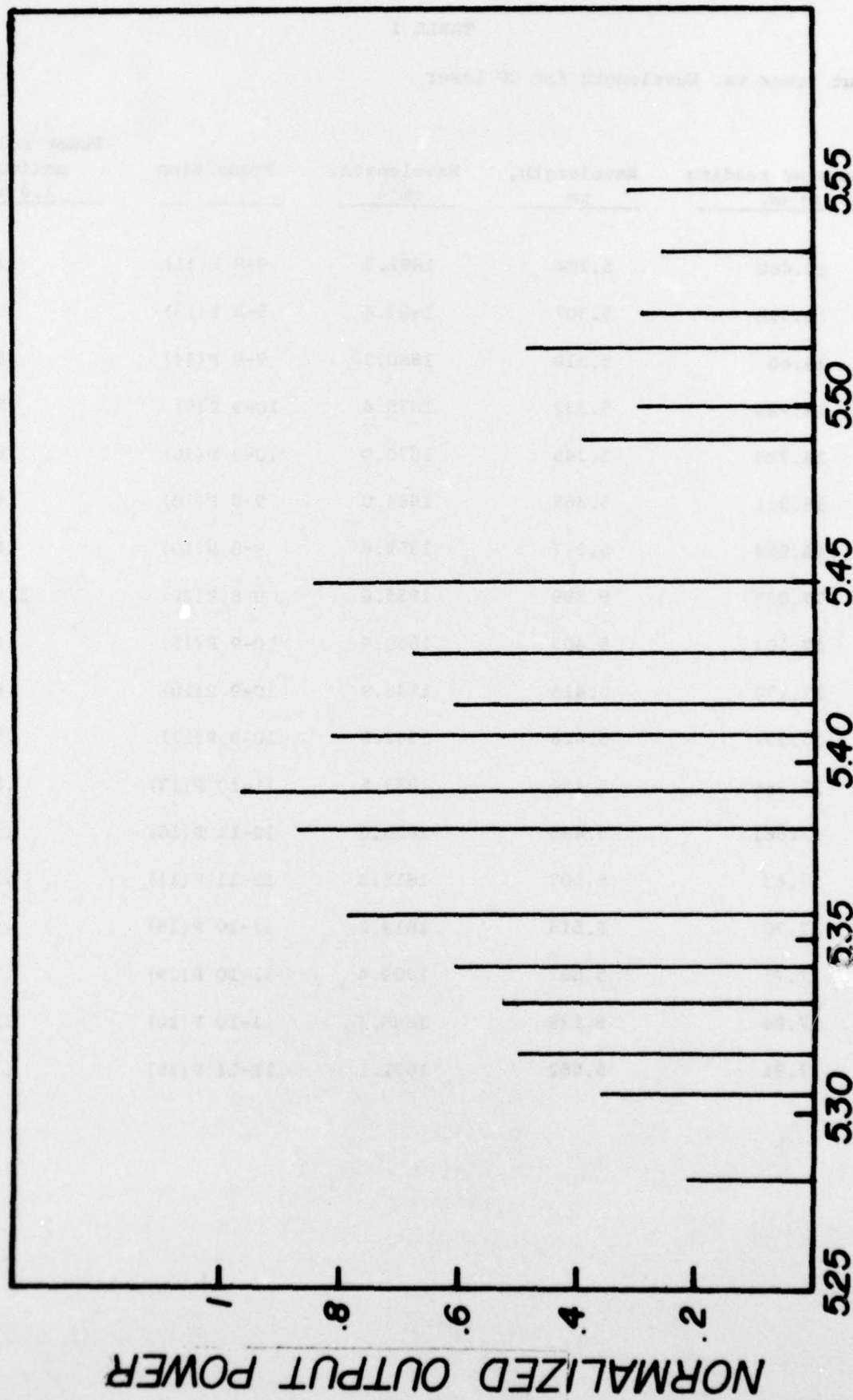


Figure 3. CARBON MONOXIDE LASER TUBE

is used to avoid contamination of the gas. Typical fill pressures range from 10 to 18 torr. The gas mixture is excited in a dc glow discharge maintained by a current regulated power supply furnishing up to 30 mA at 30 kV with a stability of .1%.⁷ Discharge current is typically 10-12 mA.

Multiline multimode peak powers of 15.5 W have been obtained in a 16 torr discharge of 11 mA at -68°C. This power output is comparable to the results of Freed⁶ who obtained a maximum power of 17.5 W in a sealed discharge at the same temperature and pressure. Single line multimode powers of up to 2.2 W have been achieved, with typical powers of 1 to 1.5 W on many lines between 5.3 and 5.6 μm . The output spectrum for a typical run is given in Figure 4 and detailed in Table I. Only those lines of sufficient intensity ($> .4$ W) to be detected in second order on an Optical Engineering CO₂ Spectrum Analyzer are shown. Many other lines at lower power levels have been observed. The spectrum shown was obtained using the 85% output coupler. The highest powers have been obtained using this mirror, while more lines are observed when the 94% reflective mirror is employed. Short term (< 1 sec) stability in the single line mode is estimated at $\pm 1.5\%$ from preliminary data. These output parameters are comparable to commercially available units such as the Molelectron IR250.⁸



WAVELENGTH IN MICRONS

Figure 4. Observed single-line multimode powers of CO laser at various wavelengths. Maximum power is 1.4 watts.

TABLE I

Output Power vs. Wavelength for CO Laser

<u>Micrometer reading in cm</u>	<u>Wavelength, μm</u>	<u>Wavelength, cm^{-1}</u>	<u>Transition</u>	<u>Power relative to maximum of 1.4 watts</u>
16.460	5.284	1892.3	9-8 P(11)	.22
16.592	5.307	1884.4	9-8 P(13)	.37
16.66	5.318	1880.3	9-8 P(14)	.52
16.725	5.332	1875.4	10-9 P(9)	.55
16.788	5.345	1870.9	10-9 P(10)	.63
16.911	5.365	1864.0	9-8 P(18)	.81
16.969	5.377	1859.8	9-8 P(19)	.89
17.035	5.389	1855.6	9-8 P(20)	1.00
17.103	5.403	1850.9	10-9 P(15)	.85
17.170	5.415	1846.9	10-9 P(16)	.63
17.237	5.426	1842.8	10-9 P(17)	.70
17.365	5.454	1833.5	11-10 P(13)	.89
17.561	5.495	1820.0	12-11 P(10)	.40
17.63	5.507	1815.8	12-11 P(11)	.31
17.70	5.515	1813.2	11-10 P(18)	.50
17.77	5.527	1809.4	11-10 P(19)	.30
17.84	5.539	1805.3	11-10 P(20)	.26
17.91	5.552	1801.1	12-11 P(15)	.31

2. cw CO₂

The CO₂ laser system is shown in Fig. 5. Several improvements have been made in the laser system during the last year as pictured in the diagram of the laser and accompanying equipment. Among the improvements made is the installation of a cooling system with chilled water. Instead of 75°F tap water, we are now using a chilled water supply at 45°F. Included also is a bubble trap to prevent any air bubbles from causing circulation problems in the cooling system. Built into the water inlet and outlet are thermocouples to allow indication of gas temperature changes caused by changes in coolant temperature. The entire vacuum system has been replaced. Rubber hose has been replaced by copper tubing wherever possible. Flow valves with linear flow patterns have been used to precisely control gas pressure and gas flow. A 60 micron filter in the gas line protects the laser tube from macroscopic particles. Six feet of rubber hose have been left on the pumping side to eliminate a ground connection from the plasma back to the pump. A two liter surgechamber has been added to damp out any gas pressure or flow variation due to the fore pump. The design can be seen in reference 9. A Marvac pump provides more pumping speed than was previously available. That coupled with larger flow rates in the valves, has extended the available total flow rates upward for more power output.

Characterization has followed three phases: the first being power as a function of current and pressure; next, came short and long term stability and finally line selectibility. The power was

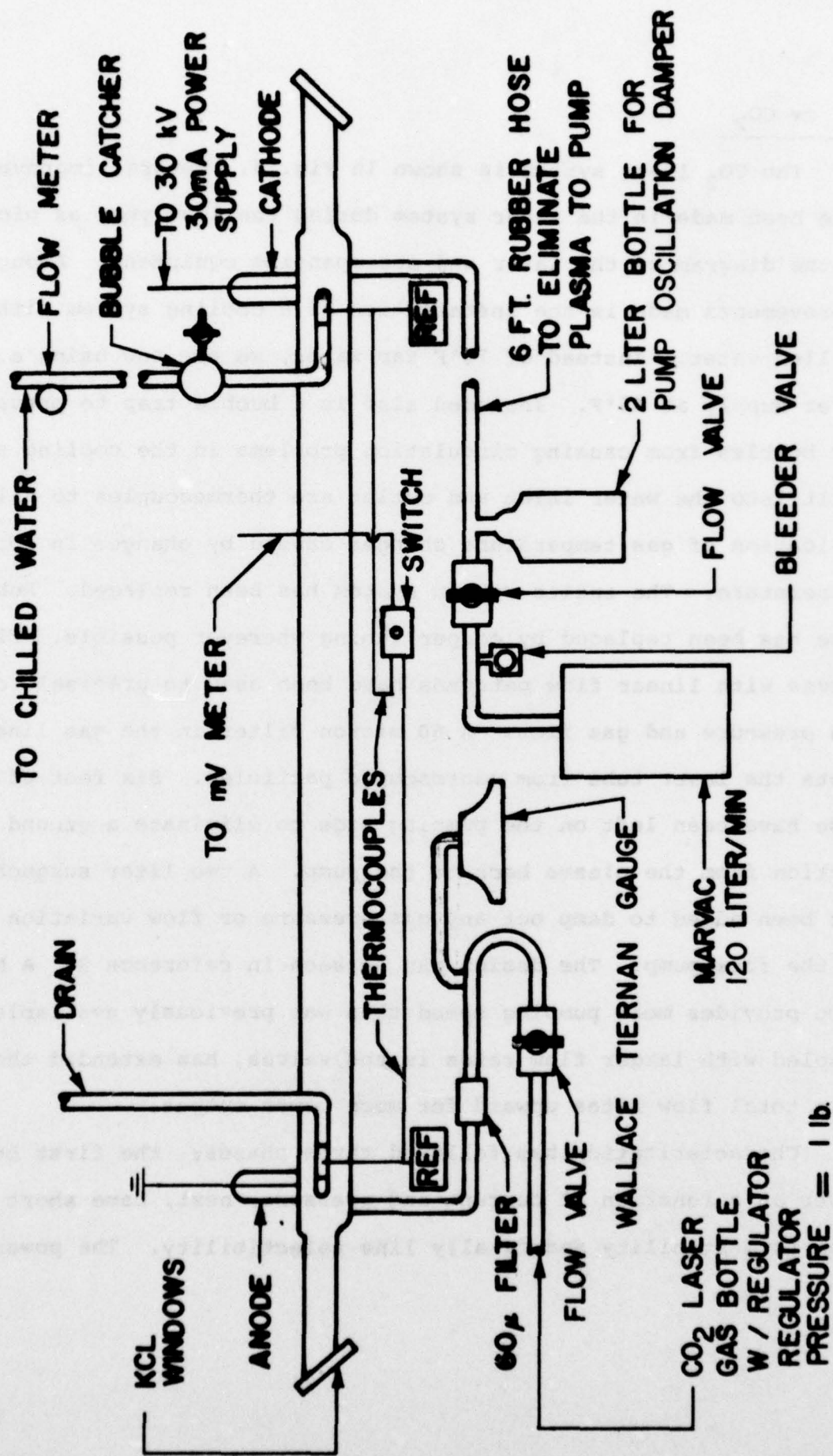


Figure 5. CO₂ LASER SYSTEM

measured with a Scien-Tech Colorimeter as current was varied from 12 mA to 28 mA using a constant current power supply, and pressure was varied from 8 torr to 30 torr where flow rates were approximately 1 liter/minute to 2 liters/minute, respectively. The gas mixture used was 15% N₂, 10% CO₂, 75% He. The maximum multimode power obtained was 39.5 watts with a grating end reflector at 26 torr and 27 mA.

Stability measurements have been completed. Short term stability was measured by a gold doped Ge detector. The laser takes from 30 minutes to 1 hour to achieve maximum short term stability. Amplitude stability for less than one second is $\pm 0.75\%$. Stability for 30 seconds is $\pm 1\%$ and for five minutes $\pm 1.5\%$. This compares very favorably with the Molelectron Model IR250 which reports stability for less than one second of $\pm 0.5\%$. After an hour period, the laser has achieved stability of $\pm 3\%$ over 5 hours as compared to $\pm 3\%$ for 4 hours for Molelectron's laser.

The last measurement is the line selectibility using a Bausch & Lomb grating blazed at 10.6 microns. The lines were viewed using an Optical Engineering CO₂ Laser Spectrum Analyzer while a beam splitter was used to take power readings from the Scien-tech Calorimeter. The power readings are for a TEM_{00q} mode. Wavelengths were observed from 9.192-10.885 microns. Seventy lines are visible with powers over two watts compared to Molelectron's 90 lines over one watt. Fifty-nine lines are available with power over 5 watts. At least 25 lines are available of 10 watts. It was found that once the laser was stable, the line would not move over a period of several hours. The laser can be left overnight and turned on without any change in wavelength.

REFERENCES

1. J. T. Yardley, Appl. Opt. 10 (8), 1760, Aug. 1971.
2. N. N. Sobolev and V. V. Sokovikov, Sov. Phys. -Usp. 16 (3), 350, Nov-Dec 1973.
3. J. W. Rich, J. Appl. Phys. 42 (7), 2719, June 1971.
4. R. M. Osgood, Jr., W. C. Eppers, Jr., and E. R. Nichols, IEEE J. Quant. Elec. QE-6 (3), 145, March 1970.
5. N. N. Sobolev and V. V. Sokovikov, Sov. J. Quant. Elec. 2 (4), 305, Jan-Feb 1973.
6. C. Freed, Appl. Phys. Letters 18, 458 (1971).
7. Dwight Maxson, D. G. Seiler, and Larry Tipton, Rev. Sci. Instrum. 46 (8), 1110 (1975).
8. Molelectron Corp., 177 N. Wolfe Road, Sunnyvale, CA 94086.
9. W. M. Swanson, Fluid Mechanics, Holt, Rinehart and Winston (New York, 1970), Chapter 15.

B. Development of a Magnetic Field Modulation

Technique for the Measurement of Oscillatory Magnetoresistance Phenomena Using Short Voltage Pulses

During the Fall 1976, a major experimental breakthrough was achieved when a new experimental technique was conceived and subsequently discovered to improve the signal-to-noise ratio in hot electron magnetophonon studies in InSb under application of high electric fields. This technique is completely adaptable to the measurement techniques used in the investigation of the laser optical biasing of the quantum transport properties of semiconductors. The capabilities of this technique were investigated by studying the extremely high resolution data obtainable on the electric-field induced hot-electron magnetophonon effect in n-InSb.

A talk was given on the technique at the March 1977 American Physical Society Meeting. Currently, this technique is being processed by the ONR patent lawyer for possible patent rights. In addition, the technique was recently published in the Review of Scientific Instruments, Vol. 48, No. 8, August, 1977, pp. 1017-1020. A copy of this paper follows below.

Magnetic field modulation technique for the study of hot carrier oscillatory magnetoresistance phenomena*

H. Kahlert[†] and D. G. Seiler

Department of Physics, North Texas State University, Denton, Texas 76203

(Received 18 November 1976; in final form, 11 February 1977)

A new experimental technique is reported which allows the detection of the oscillatory components of the magnetoresistance of semiconductors subject to high electric fields, where the pulse length must be in the submicrosecond region in order to avoid lattice heating. It uses a combination of sampling and magnetic field modulation techniques. Its capability of resolving hot-electron magnetophonon structure in n-InSb at 77 and 4.2 K for up to $N = 10$ Landau level spacings is demonstrated.

I. INTRODUCTION

Experimental investigations of oscillatory magnetoresistance phenomena under hot-electron conditions have proven to be a valuable tool for studying the effects of a high electric field on the energy distribution of electrons in semiconductors. The electric field dependence of the Shubnikov-de Haas (SdH) effect¹⁻⁴ and the magnetophonon (MP) effect⁵⁻¹⁸ have been extensively studied in a number of semiconductors.

Magnetophonon oscillations exhibit a small amplitude and are frequently superimposed on a nonoscillatory magnetoresistance background which varies quite rapidly. Thus, an accurate determination of the MP extremal positions and amplitudes is difficult even in the ohmic case. Several different experimental methods have been employed to overcome these difficulties in hot-electron studies: cancellation techniques,⁹⁻¹¹ time-derivative techniques,^{8,12-17} and third-harmonic generation combined with graphical evaluation.^{15,18} However, the poor signal-to-noise ratio involved in many of these experimental approaches tends to obscure the position and amplitude of the MP extrema.

The application of ac magnetic field modulation and phase sensitive detection techniques has been demonstrated to be a very sensitive method of investigating both the SdH effect^{19,20} and the MP effect²¹⁻²³ in the ohmic region using continuously applied small electric fields and dc currents. The sensitivity of these techniques allowed the determination of small shifts in the extremal positions of these magnetoresistance oscillations.

The purpose of this paper is to demonstrate for the first time that the magnetic field modulation technique can also be applied to pulsed measurements of the oscillatory magnetoresistance in semiconductors, where the duration of the electric field pulse has to be kept in the submicrosecond region in order to prevent lattice heating. A comparison with data obtained by conventional time-derivative techniques shows that the signal-to-noise ratio is considerably improved, allowing an unambiguous interpretation of the extremal positions. In addition, data have been gathered in lower magnetic

field regions, where the conventional techniques do not permit the extraction of the oscillatory magnetoresistance because of a poor signal-to-noise ratio.

II. EXPERIMENTAL

Figure 1 shows a block diagram of the experimental apparatus that was used in the hot-electron MP measurement. In principle, it could be used for a hot-electron SdH measurement without any alterations. It consists of three main systems: (1) the dc magnet, its power supply, and a Hall probe for monitoring the magnetic field strength, (2) the ac magnetic field modulation and lock-in amplifier system, and (3) the pulse generator, an oscilloscope for measuring the voltage across two potential probes and a sampling oscilloscope to determine the current.

The dc magnetic fields were produced by a 30-cm Varian electromagnet which was field regulated and powered by a Varian Fieldial Mark II regulator with a 10-kW power supply. The maximum field produced by the system was approximately 24 kG. A Bell Hall probe powered by a highly stable current-regulated power supply provided a voltage that drove the x-axis of the x-y recorder. Magnetic field strengths were calibrated by NMR techniques.

The ac magnetic field was produced by two Helmholtz

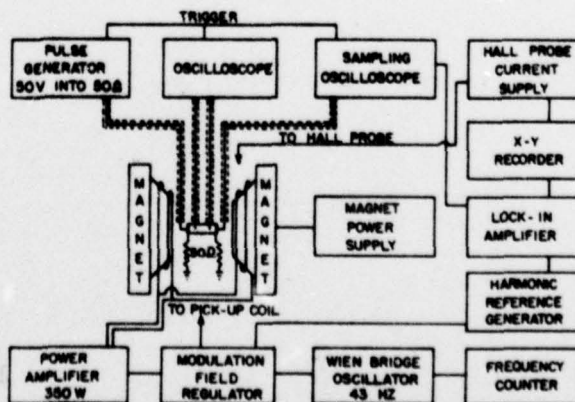


FIG. 1. Block diagram of the experimental apparatus.

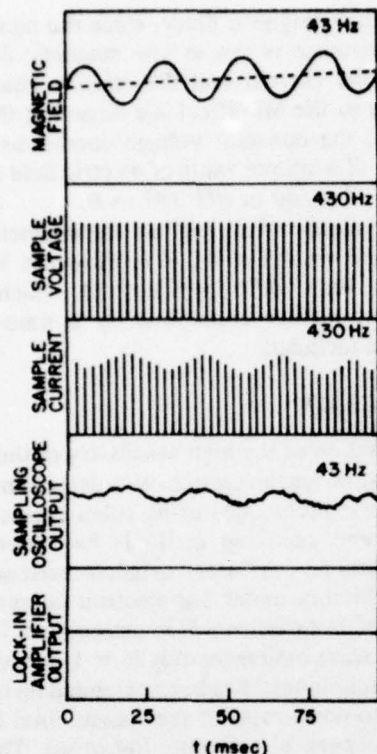


FIG. 2. Schematic time dependence of the magnetic and electric signals appearing at various components of the apparatus.

coils connected in parallel and wound on Lucite holders which were mounted around the magnet pole pieces. A Wien bridge oscillator provided a highly stable 43-Hz sinusoidal signal which was amplified by a 350-W McIntosh power amplifier. A 29- μ F capacitor was placed in series with the coils to compensate for their inductive reactance. This arrangement was capable of producing ac fields of up to 400 G peak to peak even at dc fields of up to 20 kG. Due to saturation in the magnetization of the magnet pole pieces the peak-to-peak modulation amplitude B_m decreases as the magnetic field increases. However, a modulation field regulator circuit²⁴ was used to keep the amplitude of the ac field constant. A signal proportional to B_m was induced in a pick up coil located between the pole faces of the magnet. The induced signal was used by the modulation field regulator to control the attenuation of the signal from the audio oscillator to the power amplifier so as to keep B_m constant.

The stability of the modulation frequency was monitored with a Hewlett-Packard frequency counter. There are several variables to consider in choosing a modulation field frequency: (1) clearly one does not want a harmonic or subharmonic of 60 Hz, (2) one does not want a frequency which is low enough that the Hall probe voltage produces a detectable ripple on the x-y recorder, (3) the magnitude of B_m depends upon the modulation frequency, (4) the frequency should be much less than the repetition rate of the pulse generator, and (5) the frequency affects the type of preamp used for optimum

performance of the lock-in amplifier. Consideration of the above points necessitates a compromise. A 43-Hz modulation frequency has turned out to be quite suitable.

An E-H Research Laboratory pulse generator was used to supply voltage pulses of up to 50 V across 50 Ω and of variable pulse lengths and repetition rates to the sample via a miniature coaxial cable. The rise time of these pulses was less than 12 nsec. The load of the coaxial line consisted of a network of a 50- Ω resistor in parallel with a series connection of the sample and a 50- Ω current monitoring resistor. Provided that the sample resistance exceeds 500 Ω , this network establishes constant voltage conditions that are independent of the value of the sample resistance, which can vary with increasing magnetic field. Any change of the sample resistance causes a change of the sample current and, consequently, a change in the voltage drop across the 50- Ω series resistor. This voltage drop is measured using a Tektronix 7904 mainframe oscilloscope equipped with a 7S14 sampling unit. Another oscilloscope is used to determine the voltage drop across two potential probes soldered on the sample. The sampling oscilloscope in the manual mode is set to a time position, where it displays a voltage on top of the current pulse. The output of the sampling oscilloscope, which then is proportional to the current through the sample, carries a 43-Hz modulation if the sample exhibits a nonzero magnetoresistance. This signal is then fed to a type-A preamplifier of a HR-8 PAR lock-in amplifier. For a sufficient signal-to-noise ratio the repetition rate of the pulses must be at least approximately 300 Hz. Higher repetition rates, however, substantially improve the signal-to-noise ratio and should be chosen, whenever sample heating does not influence the data.

A schematic display of the electric and magnetic signals as a function of time is shown in Fig. 2 for a pulse repetition rate exceeding the modulation frequency of the magnetic field by a factor of 10. The uppermost trace shows the modulation magnetic field superimposed on the linearly increasing dc magnetic field. The height of the sample voltage pulses shown in Fig. 2 does not depend on the magnetic field because of the circuitry used. The sample current pulses, monitored by the voltage across a 50- Ω series resistor, are modulated as

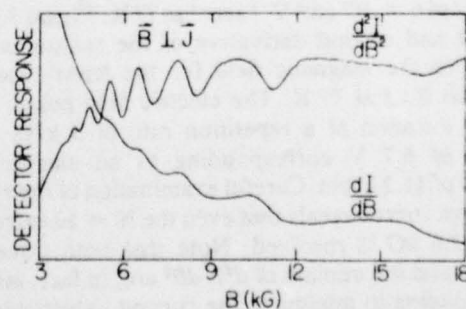


FIG. 3. First and second derivative of the current I with respect to the magnetic field B versus B for a sample of n-InSb with the current density J transverse to B . (Pulse length = 75 nsec, repetition rate = 3 kHz, $E = 11.2$ V/cm).

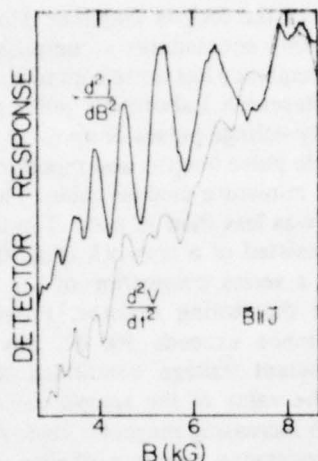


FIG. 4. Longitudinal magnetophonon effect in n-InSb at 4.2 K; full line—present technique ($E = 4.2$ V/cm, $t = 50$ nsec); dashed line—data from Ref. 14, time-derivative technique ($E = 0.88$ V/cm, $t = 200$ nsec).

shown in Fig. 2 if the resistance is an increasing function of magnetic field. The output of the sampling oscilloscope is thus modulated and carries the essential information about the dependence of the resistance on the magnetic field along with noise. The lock-in amplifier when set to 43-Hz phase sensitively detects the 43-Hz component of the sampling oscilloscope output signal and demodulates it to a dc voltage. If a linear relationship exists between the sample resistance and the magnetic field, the dc output of the lock-in amplifier will be essentially constant, as shown in the bottom part of Fig. 2. Any nonlinearity changes the amplitude of the ac component of the sampling oscilloscope output and therefore a first derivative of the magnetoresistance $R(B)$ curve is obtained. By setting the lock-in amplifier to the second harmonic frequency (86 Hz) the second derivative of the magnetoresistance is attained.

III. RESULTS

The capability of the method described in the previous section was proved by resolving MP structure in the transverse and longitudinal magnetoresistance of n-InSb at 77 and 4.2 K, respectively. The n-InSb sample had a carrier concentration of $n = 1 \times 10^{14}$ cm $^{-3}$ and a mobility of 6×10^5 cm 2 V $^{-1}$ sec $^{-1}$ at 77 K. Figure 3 shows the first and second derivative of the resistance with respect to the magnetic field for the transverse configuration $B \perp J$ at 77 K. The electric field pulses had a 75-nsec duration at a repetition rate of 3 kHz and a voltage of 6.7 V corresponding to an electric field strength of 11.2 V/cm. Careful examination of the second derivative curve reveals that even the $N = 10$ extremum at $B \sim 3.6$ kG is resolved. Note that both traces are inverted and the minima of d^2I/dB^2 are, in fact, maxima corresponding to minima in the current, which occur at the maxima of the transverse magnetoresistance. We would like to emphasize that the method applied to the transverse MP effect is especially suited to detecting

extrema at low magnetic fields, since the nonoscillatory magnetoresistance is low at low magnetic fields. Consequently, the current and the relative change in the current due to the MP effect are largest at these fields. In addition, the constant voltage conditions allow the assignment of a unique value of electric field strength to a full trace of dI/dB or d^2I/dB^2 vs B .

The dependence of d^2I/dB^2 on the magnetic field for the configuration $B \parallel J$ at 4.2 K is shown in Fig. 4. For comparison, data taken from Ref. 14, which were obtained under similar conditions by a time-derivative method, are included.

IV. DISCUSSION

A combination of the high sensitivity of the magnetic field modulation and phase-sensitive detection technique with fast pulse techniques using submicrosecond pulse generation and sampling methods has provided high resolution data on oscillatory magnetoresistance effects in semiconductors under hot-electron conditions. The resolution of hot-electron MP extrema at 77 K with $B \perp J$, which was possible for only $N = 1, 2, 3$, using time-derivative techniques,⁹ has been extended up to $N = 10$. The signal-to-noise ratio of the longitudinal MP effect at 4.2 K has been significantly improved. This advantage compared to conventional techniques is mainly caused by introducing the signal recovery capabilities of the phase-sensitive lock-in amplifier applied to the analog output of a fast sampling oscilloscope.

A disadvantage of this method may be the lower limit for the pulse repetition frequency, which is in the range of about 5–10 times the frequency of the ac magnetic field.

Currently discussed topics like the occurrence of spin-flip extrema in the low-temperature hot-electron MP effect in n-InSb¹⁰ and in the shift of the transverse MP extrema in n-InSb with applied electric field⁹ should be reexamined in view of the high resolution potentially obtainable by this method.

ACKNOWLEDGMENTS

We are grateful to Dr. A. E. Stephens for his help in setting up parts of the equipment.

* Work supported in part by the Office of Naval Research.

† On leave from Ludwig Boltzmann Institut für Festkörperphysik and Institut für angewandte Physik, Universität Wien, A-1090 Vienna, Austria.

¹ G. Bauer and H. Kahlert, in *Proceedings of the International Conference on the Physics of Semiconductors*, Cambridge, 1970, edited by S. P. Keller, J. C. Hensel, and F. Stern (U.S. Atomic Energy Commission, Oak Ridge, 1970), p. 65.

² H. Kahlert and G. Bauer, *Phys. Status Solidi B* **46**, 535 (1971).

³ G. Bauer and H. Kahlert, *Phys. Rev. B* **5**, 566 (1972).

⁴ H. Kahlert and G. Bauer, *Phys. Rev. B* **7**, 2670 (1973).

⁵ R. A. Stradling and R. A. Wood, *J. Phys. C* **3**, 2425 (1970).

⁶ R. A. Stradling, in *Proceedings of the 11th International Conference on the Physics of Semiconductors*, Warsaw, 1972, edited by M. Miasek (PWN-Polish Scientific Publishers, Warsaw, 1972), p. 261.

⁷ P. G. Harper, J. W. Hodby, and R. A. Stradling, *Rep. Prog. Phys.* **36**, 1 (1973).

- ⁸ R. L. Peterson, in *Semiconductors and Semimetals*, edited by R. K. Willardson and A. C. Beer (Academic, New York, 1975), Vol. 10, p. 221.
- ⁹ R. C. Curby and D. K. Ferry, in *Proceedings of the 11th International Conference on the Physics of Semiconductors, Warsaw, 1972*, edited by M. Miasek (PWN-Polish Scientific Publishers, Warsaw, 1972), p. 312.
- ¹⁰ W. Zawadzki, G. Bauer, W. Racek, and H. Kahlert, *Phys. Rev. Lett.* **35**, 1098 (1975).
- ¹¹ W. Racek and G. Bauer, *Phys. Rev. Lett.* **37**, 1032 (1976).
- ¹² M. M. Aksel'rod, V. P. Lugov'kh, R. V. Pomortsev, and M. Tsidilkovskii, *Sov. Phys. Solid State* **11**, 81 (1969).
- ¹³ G. Bauer, E. Erking, H. Kahlert, and W. Racek, *J. Phys. E* **6**, 186 (1973).
- ¹⁴ W. Racek, H. Kahlert, G. Bauer, and P. Kocevar, in *Proceedings of the 12th International Conference on the Physics of Semiconductors, Stuttgart 1974*, edited by M. Pilkuhn (Teubner, Stuttgart, 1974), p. 849.
- ¹⁵ T. Shirakawa, C. Hamaguchi, and J. Nakai, *J. Phys. Soc. Jpn.* **35**, 1098 (1973).
- ¹⁶ M. Ito, T. Shirakawa, C. Hamaguchi, and J. Nakai, *Solid State Commun.* **17**, 717 (1975).
- ¹⁷ T. Shirakawa, M. Ito, K. Kasai, and C. Hamaguchi, *Phys. Lett. A* **58**, 123 (1976).
- ¹⁸ C. Hamaguchi, T. Shirakawa, T. Yamashita, and J. Nakai, *Phys. Rev. Lett.* **28**, 1129 (1972).
- ¹⁹ D. G. Seiler and W. M. Becker, *Phys. Rev.* **183**, 784 (1969).
- ²⁰ D. G. Seiler and K. L. Hathcox, *Phys. Rev. B* **9**, 648 (1974).
- ²¹ D. G. Seiler, D. L. Alsup, and R. Muthukrishnan, *Solid State Commun.* **10**, 865 (1972).
- ²² D. G. Seiler and F. Addington, *Rev. Sci. Instrum.* **43**, 749 (1972).
- ²³ D. G. Seiler, T. J. Joseph, and R. D. Bright, *Phys. Rev. B* **9**, 716 (1974).
- ²⁴ R. J. Jirberg, *Rev. Sci. Instrum.* **40**, 173 (1969).

V. EXPERIMENTAL RESULTS

A. Magnetophonon Studies

Several studies have been done on the magnetophonon (MP) effect in n-InSb the past year. This can be divided into the low electric field region and the high electric field region.

1. Low Electric Field Region

Enhanced resolution by sensitive measurement techniques allowed several studies to be done. As a result, two papers will be published on this work. To best summarize this work, we present the title of the paper and reproduce the corresponding abstract.

OBSERVATION OF MAGNETOPHONON STRUCTURE

IN

DEGENERATE n-InSb

ABSTRACT

We report the observation of magnetophonon structure in the transverse magnetoresistance of degenerate n-InSb at 77 K in a sample of concentration $7.5 \times 10^{15} \text{ cm}^{-3}$. The positions of the resistance maxima appear at higher magnetic fields than those found in pure ($\leq 10^{14} \text{ cm}^{-3}$) samples.

THE MAGNETOPHONON EFFECT IN A NONPARABOLIC

BAND: n-TYPE InSb

ABSTRACT

Measurements of the transverse Ohmic magnetophonon effect have been performed at 77 K in a set of samples of n-InSb having carrier concentrations in the range from $n = 5 \times 10^{13} \text{ cm}^{-3}$ to $n = 7 \times 10^{16} \text{ cm}^{-3}$. With increasing doping, the minima in the second derivative of the resistance with respect to the magnetic field are shifted to higher magnetic fields. Even in the purest samples the values of the resonant magnetic fields for harmonic numbers up to $N = 12$ can only be explained if the contributions of spin-conserving transitions involving both $L = 0$ spin levels and spin-split Landau levels with $L > 0$ are taken into account. These transitions occur at magnetic fields which are higher than the fields for the $L = 0$ lower spin level transition because of the nonparabolicity of the InSb-conduction band. A superposition of Lorentzian lines with an empirically determined halfwidth $\Delta(N)$ proportional to the harmonic number N and weighted with the value of the Fermi distribution function at the energy of the lower level is shown to

give a good fit to the data yielding a band-edge effective mass of $m_0^* = 0.0138 m_0$. In higher doped samples, the shift of the extrema to higher magnetic fields is partially caused by the larger value of the damping parameter, because of the lower mobility. After applying an appropriate correction to the extremal positions of the high concentration samples, a shift remains, which qualitatively can be explained by the increasing contribution of higher order transitions because of the higher population of these levels. Finally, the shifts in extremal position as a consequence of an increased electron temperature, e.g., induced by application of electric fields or photoexcitation, are discussed within the framework of this model.

2. High Electric Field Region

As stated earlier in the Experimental Work Section, Part B, during the past year a new technique was developed for measuring oscillatory magnetoresistance phenomena using submicrosecond voltage pulses. Consequently, this magnetic field modulation technique enabled high resolution data on the electric field dependence of the MP oscillations in n-InSb to be obtained.

One paper will be published which will contain the results which are summarized below by the title and abstract of the paper.

ELECTRIC FIELD DEPENDENCE OF THE
POSITIONS AND AMPLITUDES OF MAGNETOPHONON
OSCILLATIONS IN n-InSb AT 77 K

ABSTRACT

The influence of pulsed electric fields on the magnetophonon structure in the transverse and longitudinal magnetoresistance of n-InSb at 77 K has been reexamined using a magnetic field modulation technique. For the transverse configuration, a shift to higher magnetic fields with increasing electric field is observed for the resistance maxima up to $N = 8$. The amplitudes decrease monotonously and disappear at about 60V/cm for $N = 3$. In the longitudinal case, the extrema shift to lower magnetic fields as the electric field is increased. In contrast to the transverse case, the amplitudes increase by a factor of 1.8 up to 15V/cm, and then either decrease or become saturated, depending on the harmonic number of the extremum under consideration. These experimental results are discussed within the context of calculations based on a quantum kinetic equation approach and predictions obtained from a simplified analytical theory.

B. Laser Induced Changes in the Shubnikov-de Haas Effect

Much progress has been made during the past year and as such we shall try to cover this part as comprehensively as possible. This part is conveniently divided into two sections, Pulsed dc Method and Magnetic Field Modulation Method, according to the method used in recording the Shubnikov-de Haas (SdH) oscillations.

1. Pulsed dc Method

The first direct observation of CO₂ laser-induced hot electrons in degenerate n-InSb was carried out using a pulsed dc electric field technique as shown in Fig. 6. The laser radiation is pulsed with a low duty cycle to prevent lattice heating. The pulsed dc electric field is synchronized with the optical pulse and the response of the laser-induced hot electrons is measured by sampling oscilloscope techniques.

Shubnikov-de Haas measurements were carried out on a sample of n-InSb with a concentration $1.4 \times 10^{15} \text{ cm}^{-3}$ at 1.5 K and with $\vec{B} \parallel \vec{J}$. The optical pulse used was 3 μsec wide and was produced from a cw CO₂ laser beam at a repetition rate of 166 Hz by a mechanical chopper. The ohmic voltage pulse had a duration of 20 nsec. The response of the electrons was measured through a pair of voltage probes, amplified, and displayed on a Tectronix 7904/7S14 sampling oscilloscope. For these measurements, the output of the sampling oscilloscope was recorded directly on an X-Y recorder as shown in Fig. 6.

The electron temperature was measured by comparing the amplitude of the SdH oscillations taken under laser heating conditions with those taken under equilibrium conditions at various lattice

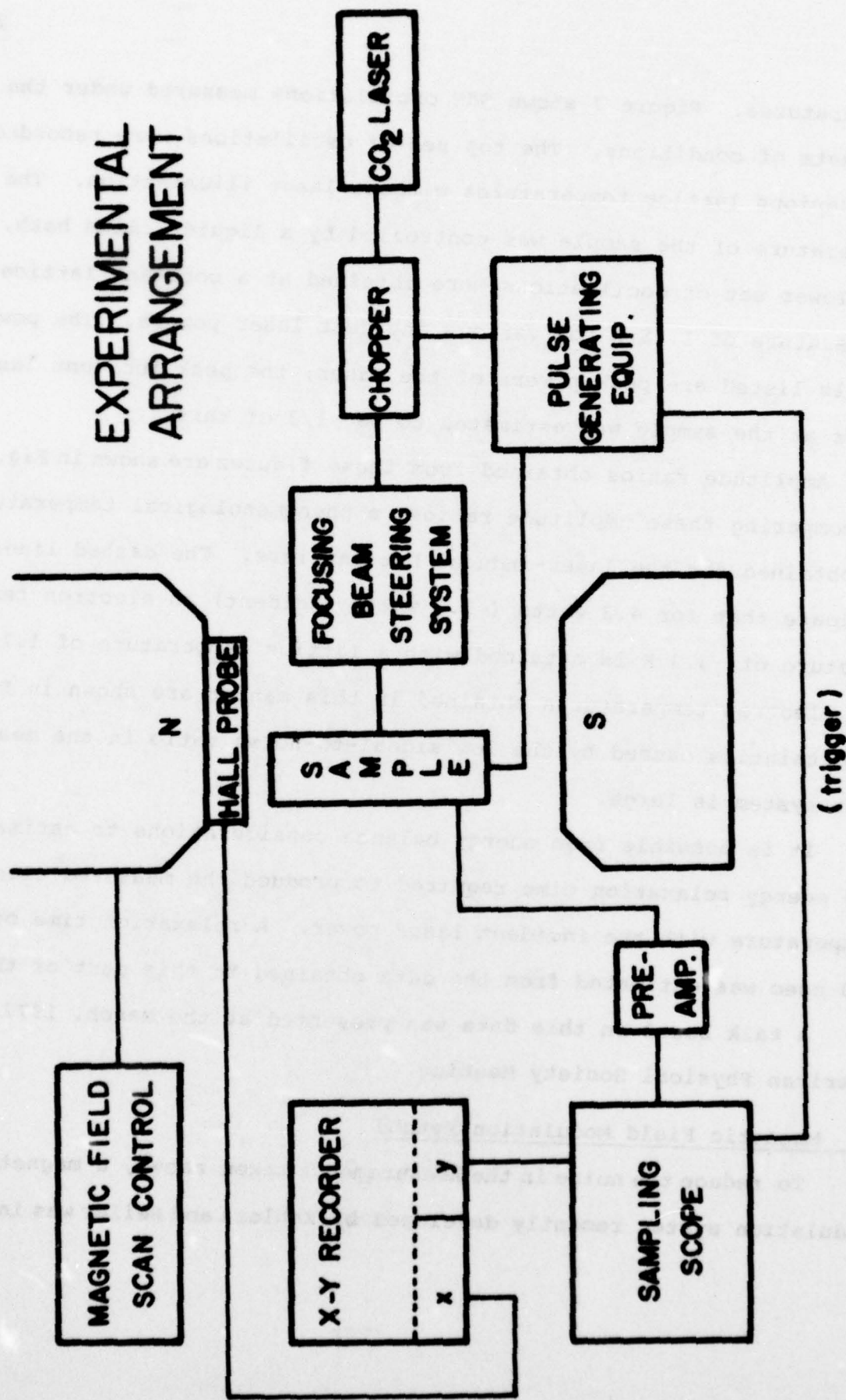


Figure 6. Block Diagram of Experimental Apparatus Used in Pulsed dc Method.

temperatures. Figure 7 shows SdH oscillations measured under the two sets of conditions. The top set of oscillations were recorded for various lattice temperatures without laser illumination. The temperature of the sample was controlled by a liquid helium bath. The lower set of oscillations were obtained at a constant lattice temperature of 1.75 K for various incident laser powers. The power levels listed are peak powers of the laser; the peak incident laser power at the sample was estimated to be $\sim 1/3$ of this.

Amplitude ratios obtained from these figures are shown in Fig. 8. By comparing these amplitude ratios, a phenomenological temperature is obtained for the laser-induced hot carriers. The dashed lines indicate that for 4.2 watts (~ 1.3 watts incident) an electron temperature of ~ 3.3 K is obtained with a lattice temperature of 1.75 K. The electron temperatures obtained in this manner are shown in Fig. 9. Uncertainties caused by the low signal-to-noise ratio in the measurement system is large.

It is possible from energy balance considerations to estimate the energy relaxation time required to produce the measured electron temperature with the incident laser power. A relaxation time of ~ 10 nsec was estimated from the data obtained in this part of the study.

A talk based on this data was presented at the March, 1977, American Physical Society Meeting.

2. Magnetic Field Modulation Method

To reduce the noise in the measurements taken above, a magnetic field modulation system recently developed by Kahlert and Seiler was incorporated

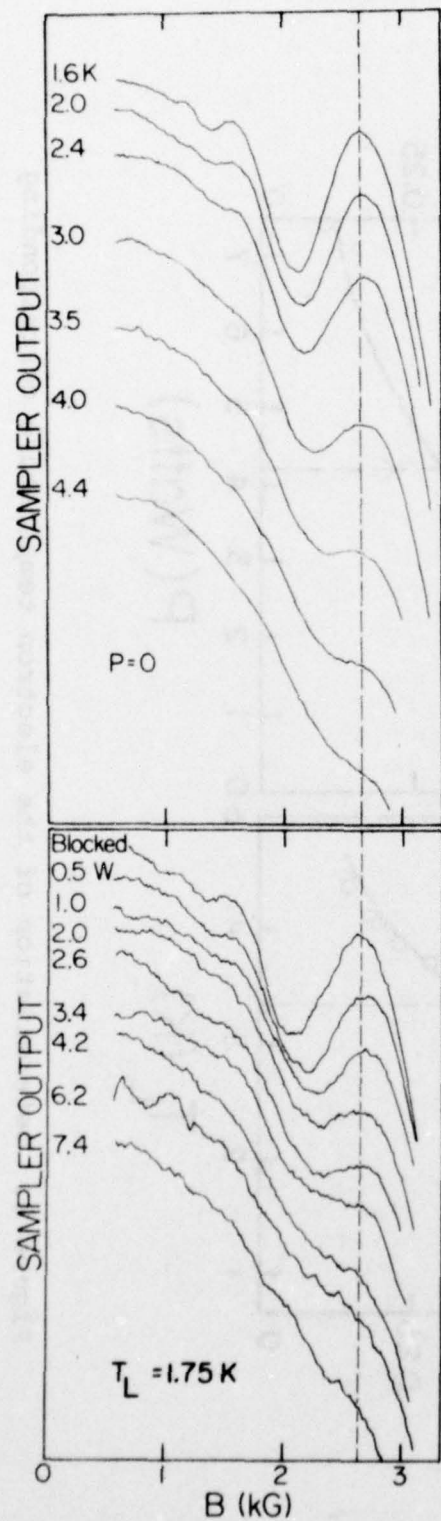


Figure 7. Top Half: Temperature dependence in n-InSb at zero laser power; Bottom half: Dependence of SdH oscillations on the peak power of a Co_2 laser pulse. Both sets of data were taken with a sampling oscilloscope.

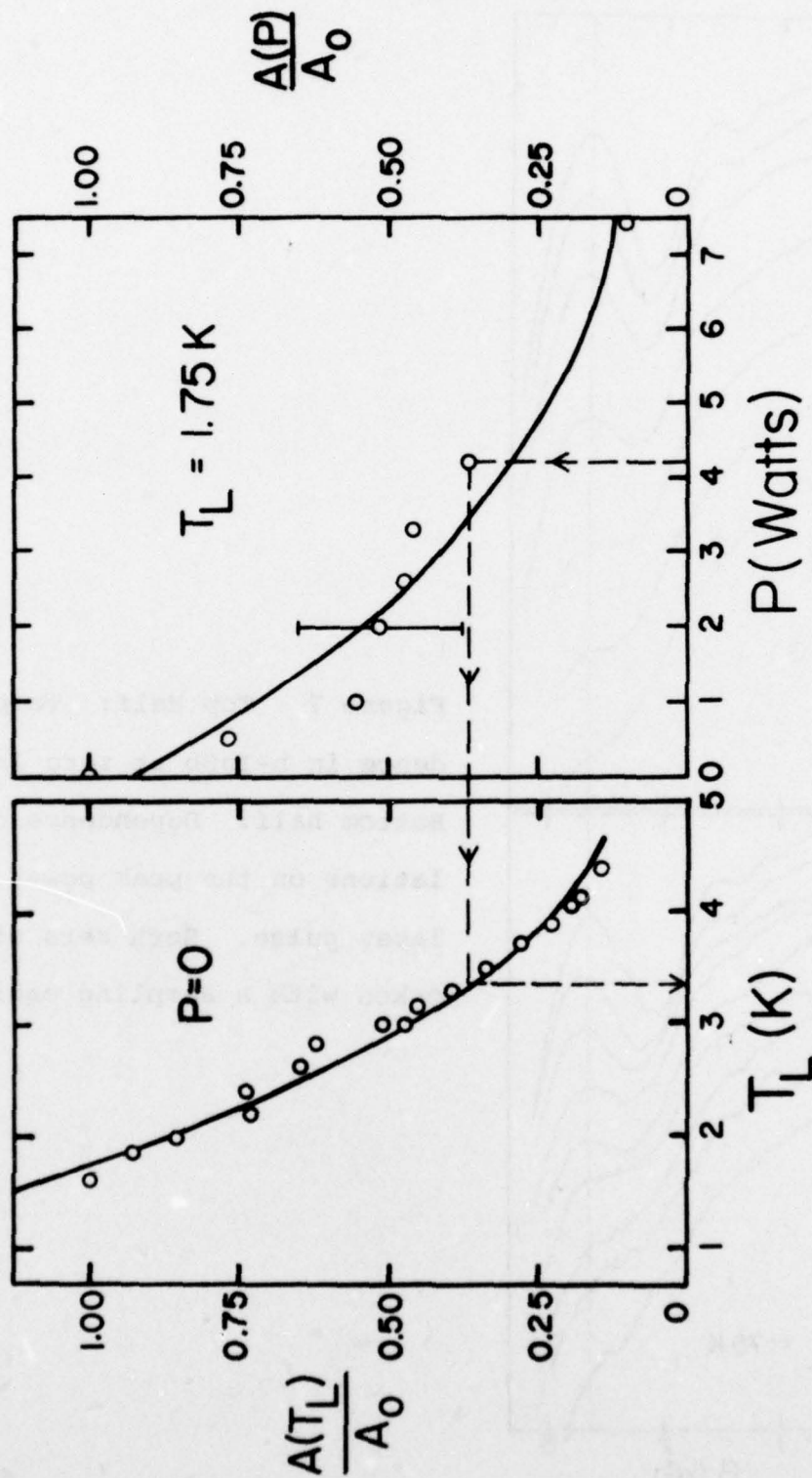


Figure 8. Determination of the electron temperature corresponding to certain laser powers and at a magnetic field of about 2 kG; Left-hand Side: variation of the normalized amplitude with lattice temperature T_L ; Right-hand Side: dependence of normalized amplitude on laser power at a fixed lattice temperature.

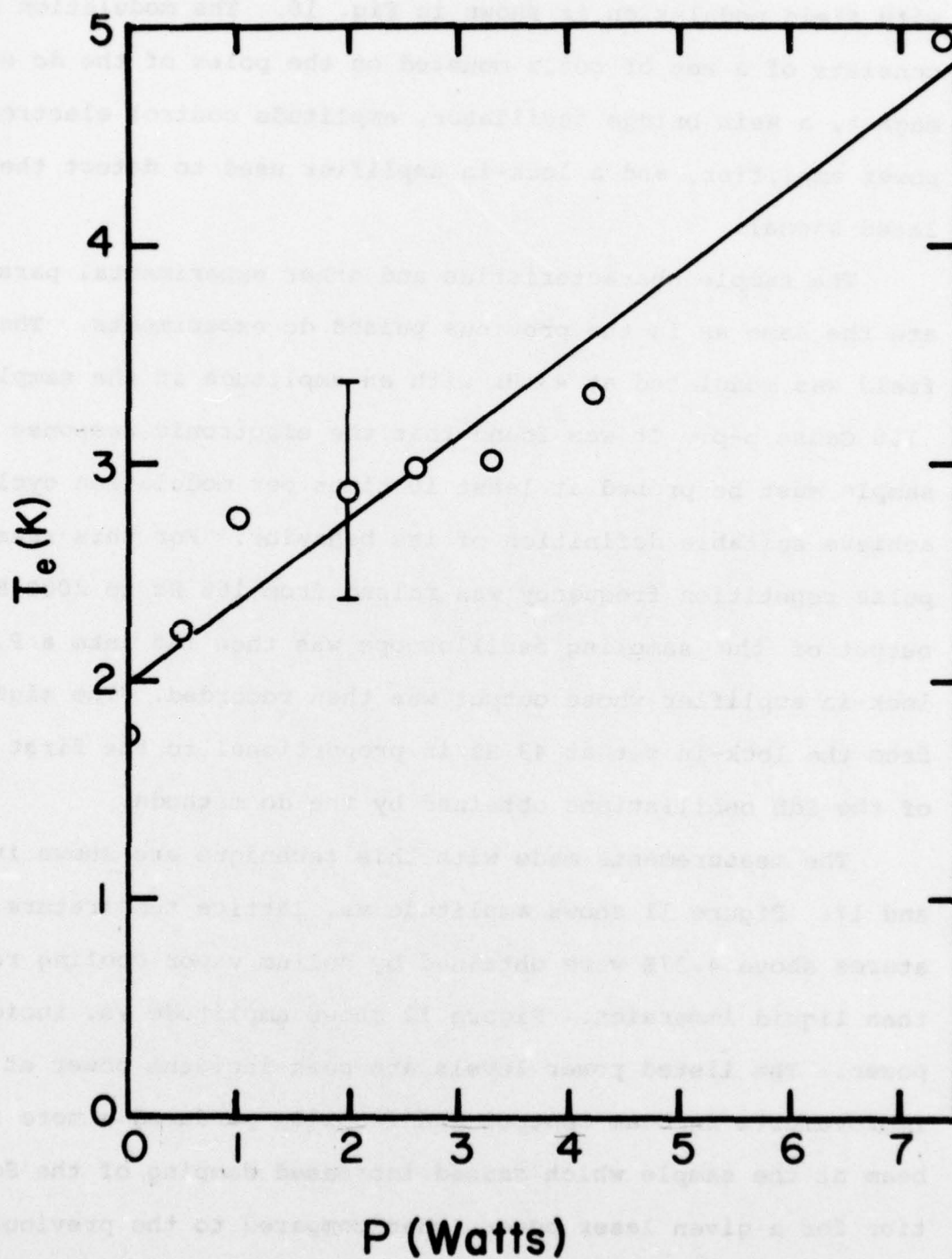


Figure 9. Dependence of the CO_2 laser-induced electron temperature on the peak value of the laser pulse at a fixed lattice temperature of 1.75 K. Actual power incident on the sample is about one-third of that given.

into the experimental arrangement. A block diagram of the experiment with field modulation is shown in Fig. 10. The modulation system consists of a set of coils mounted on the poles of the dc electromagnet, a Wein bridge oscillator, amplitude control electronics, power amplifier, and a lock-in amplifier used to detect the modulated signal.

The sample characteristics and other experimental parameters are the same as in the previous pulsed dc experiments. The magnetic field was modulated at 43 Hz with an amplitude at the sample of 150 Gauss p-p. It was found that the electronic response of the sample must be probed at least 10 times per modulation cycle to achieve suitable definition of its behavior. For this reason the pulse repetition frequency was raised from 166 Hz to 2000 Hz. The output of the sampling oscilloscope was then fed into a P.A.R. HR-8 lock-in amplifier whose output was then recorded. The signal derived from the lock-in set at 43 Hz is proportional to the first derivative of the SdH oscillations obtained by the dc methods.

The measurements made with this technique are shown in Figs. 11 and 12. Figure 11 shows amplitude vs. lattice temperature, temperatures above 4.37K were obtained by helium vapor cooling rather than liquid immersion. Figure 12 shows amplitude vs. incident laser power. The listed power levels are peak incident power at the sample. Improvements in beam control and focusing produced a more intense beam at the sample which caused increased damping of the SdH oscillation for a given laser power, when compared to the previous data shown in Fig. 7. Figs. 13 and 14 show the amplitude ratios and

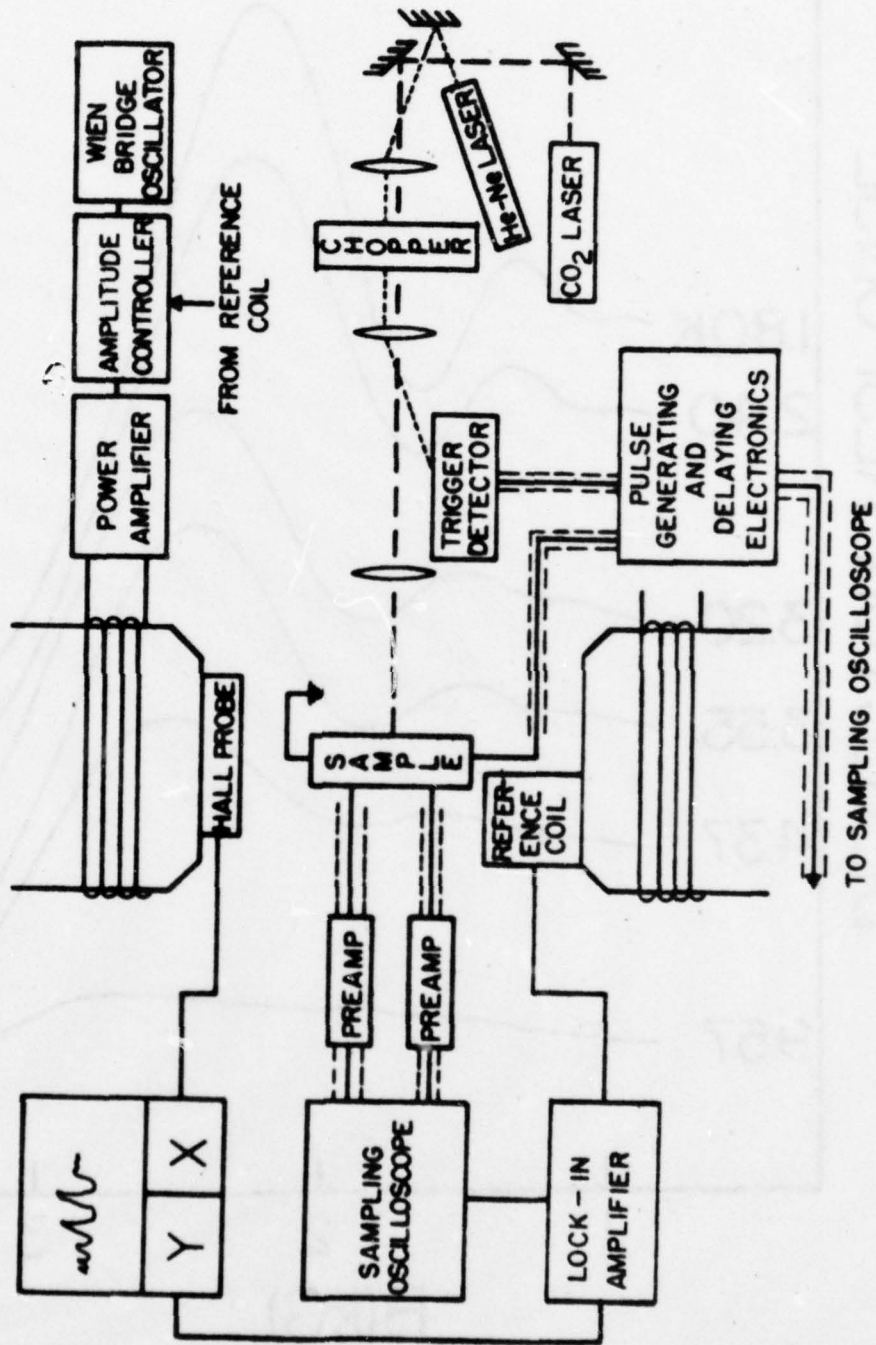


Figure 10. Block diagram of experimental apparatus used in the magnetic field modulation method.

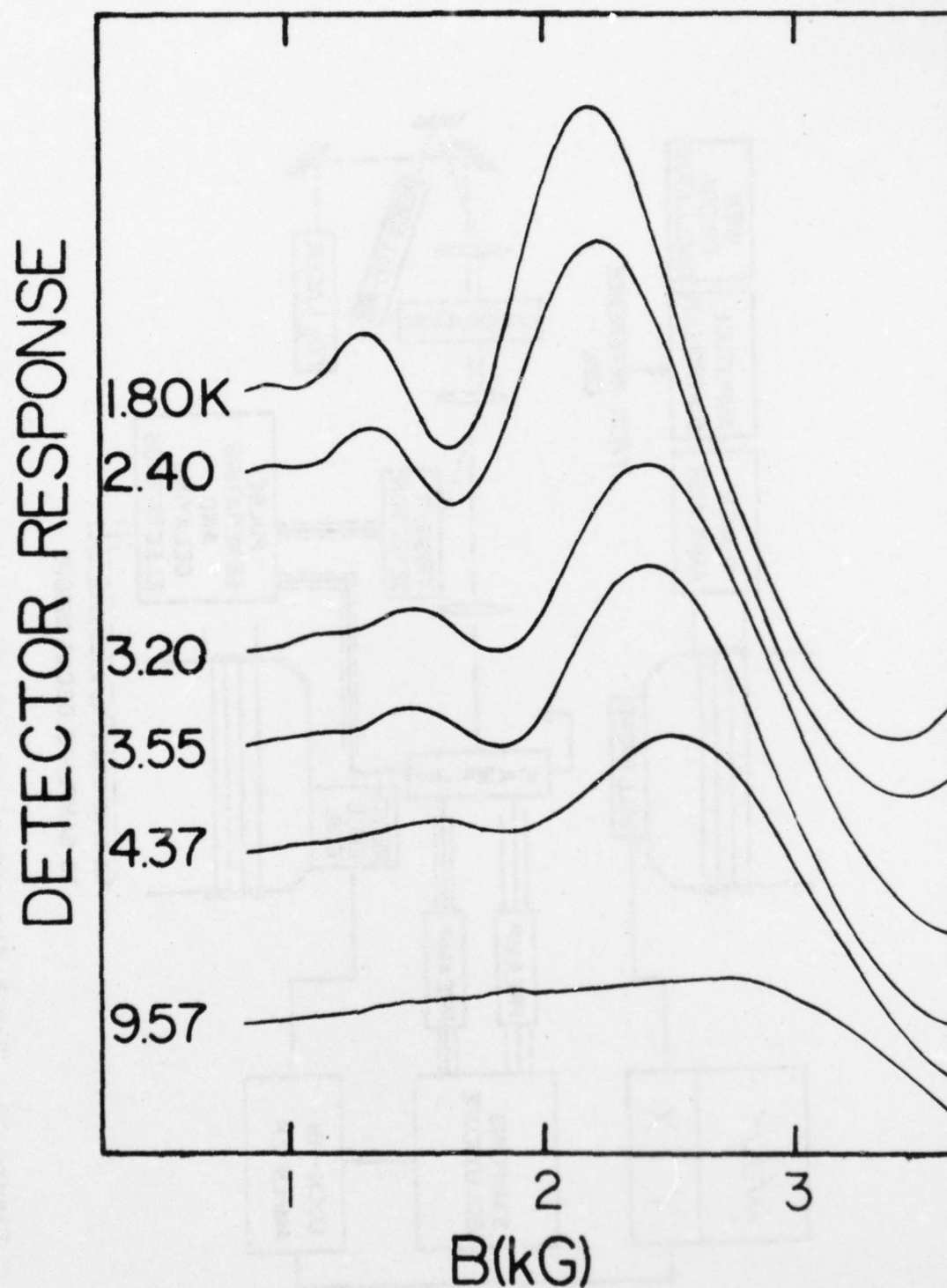


Figure 11. SdH oscillatory magnetoresistance for several lattice temperatures taken while detecting at the first harmonic of the modulation frequency (no laser illumination).

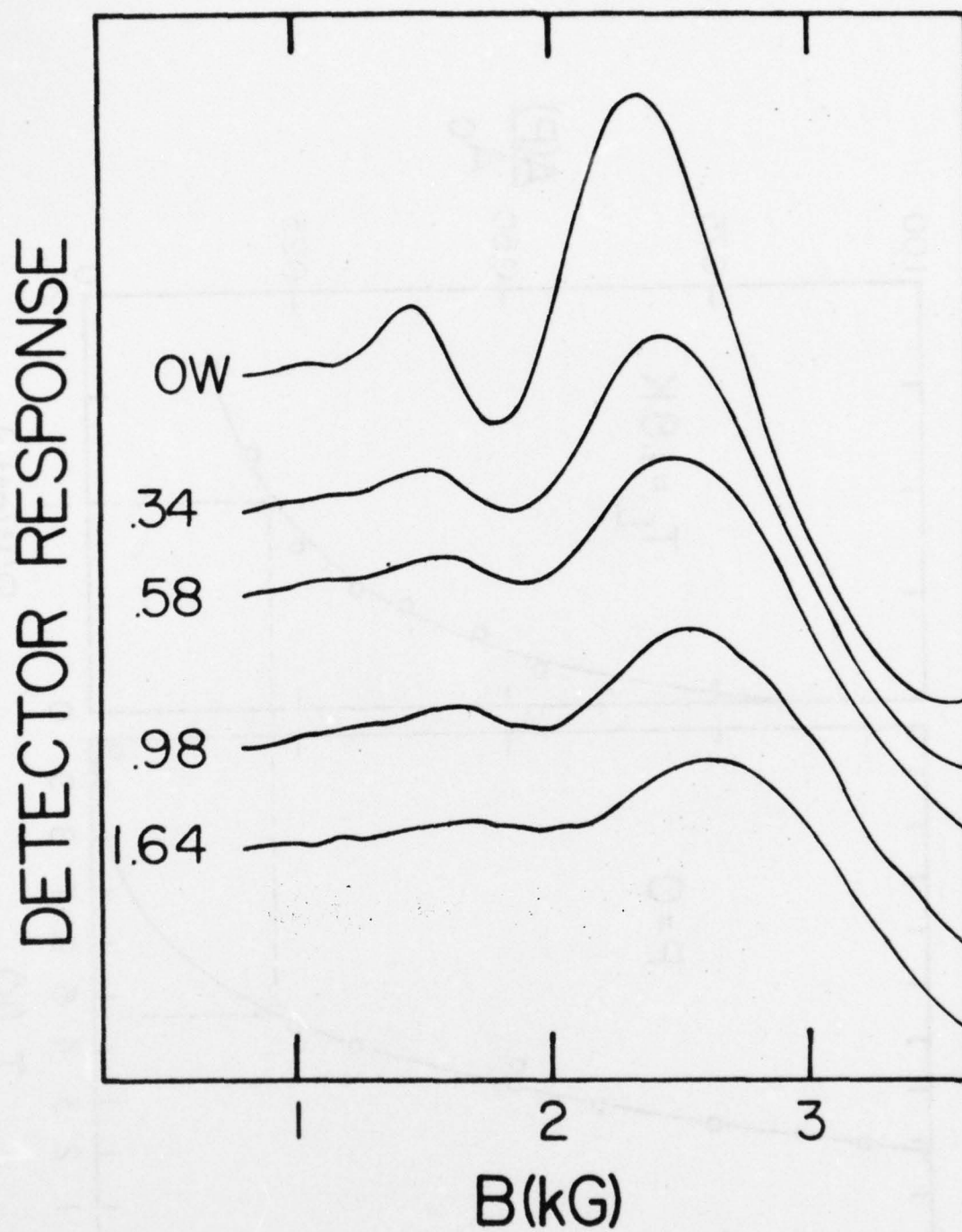


Figure 12. SdH oscillations for various incident laser powers at a constant lattice temperature of 1.8 K. Power levels listed are peak incident power at the sample.

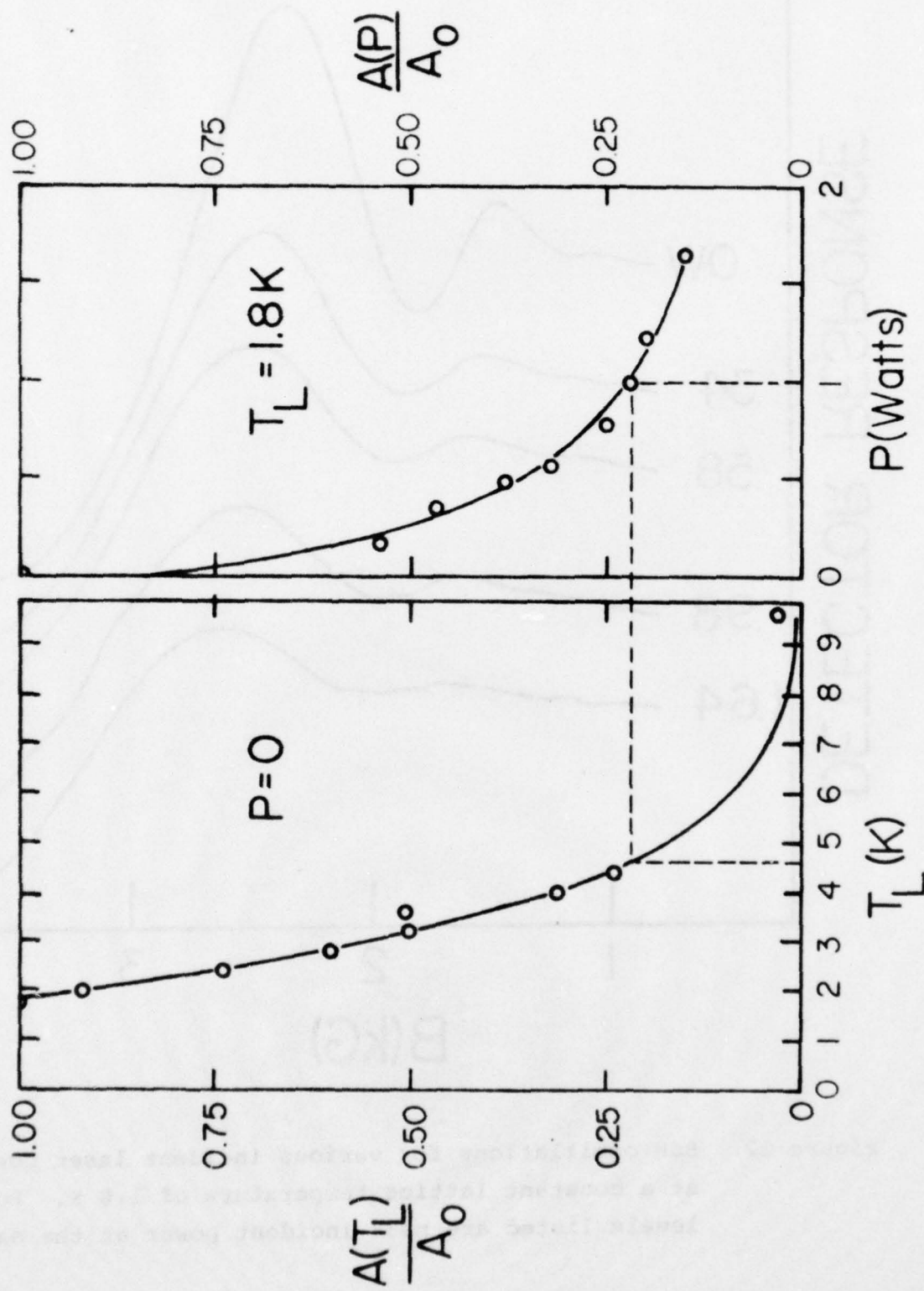


Figure 13. SdH amplitude ratios versus lattice temp (left) and versus incident laser power (right).

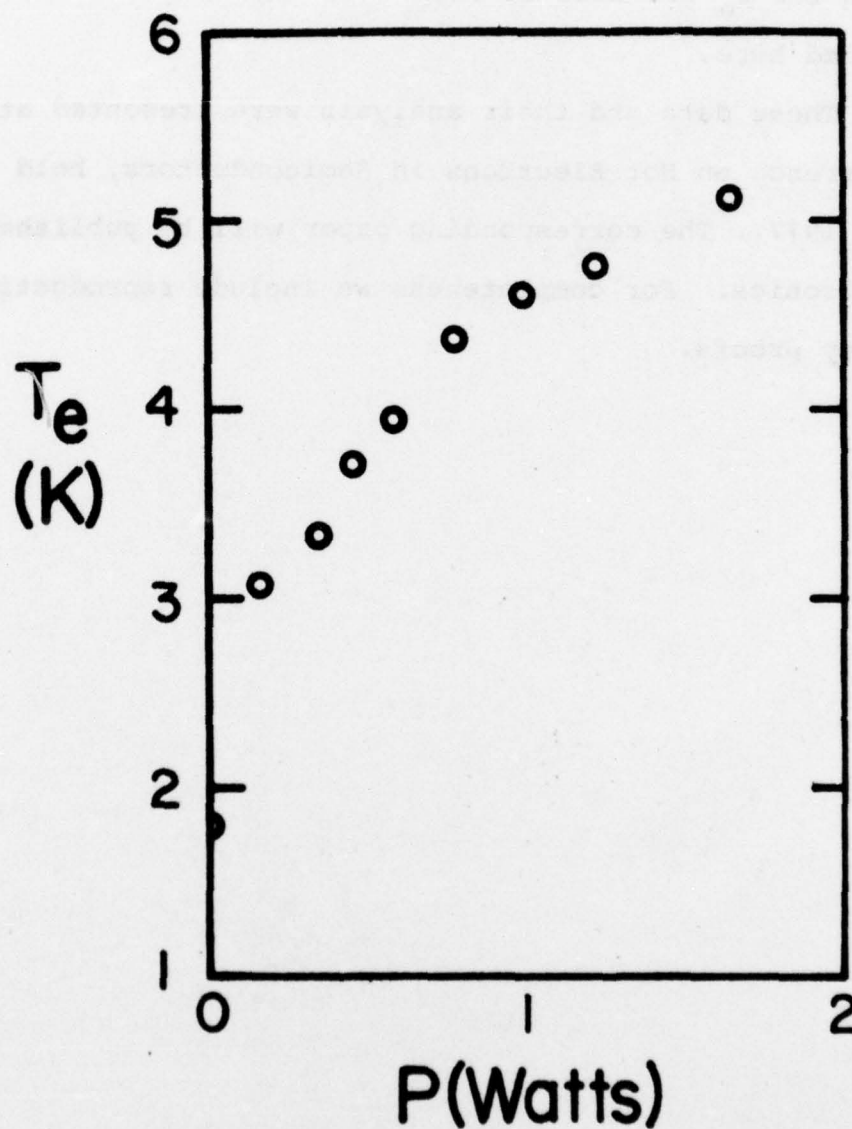


Figure 14. Electron temperature T_e versus laser power.

electron temperatures obtained from the oscillations in Figs. 11 and 12. The electron temperatures obtained in this study show a slight fall-off at higher laser powers. This effect yields a decrease in energy relaxation time with increasing laser power for calculations based on energy balance considerations. Values calculated for T_e are near 25 nsec over the range of laser powers studied here.

These data and their analysis were presented at the International Conference on Hot Electrons in Semiconductors, held at NTSU, July 6-8, 1977. The corresponding paper will be published in Solid State Electronics. For completeness we include reproductions of the galley proofs.

CO₂ LASER-INDUCED HOT ELECTRON EFFECTS IN *n*-InSb†

B. T. MOORE, D. G. SEILER and H. KAHNERT‡

Department of Physics, North Texas State University, Denton, TX 76203, U.S.A.

Abstract—The influence of a 3- μ sec wide CO₂ laser pulse on the Shubnikov-de Haas (SdH) effect in a $1.4 \times 10^{15} \text{ cm}^{-3}$ sample of *n*-InSb has been investigated at a lattice temperature of 1.8 K. During the time the sample is illuminated the SdH amplitudes are found to decrease with increasing laser power. For a peak incident power of about 1 watt, the SdH oscillatory behavior corresponds to that measured at a lattice temperature of 4.6 K for the non-illuminated sample. These results form the first direct and quantitative evidence for electron heating induced by CO₂ laser radiation and permit the evaluation of a phenomenological energy relaxation time.

1. INTRODUCTION

Hot electrons in InSb created by d.c. electric fields have been extensively studied by a variety of experiments, both for nondegenerate and degenerate statistics. However, for the case of optical heating, much less information is available. In pure ($<10^{14} \text{ cm}^{-3}$) samples of InSb illuminated by long wavelength radiation, free carrier absorption is known to cause an increase in the mean energy of the electron gas as observed by changes in conductivity resulting from a mobility variation[1, 2]. Determination of electron temperatures from photoconductivity data depends upon the assumptions made concerning the dominant scattering mechanisms. In addition, this technique is not as sensitive in degenerate samples of InSb since the mobility is not strongly dependent upon temperature.

In this paper, we present the first direct measurements of CO₂-laser induced hot electron temperatures in degenerate *n*-type InSb. These measurements involve determining the amplitude of the Shubnikov-de Haas (SdH) oscillations which are strongly dependent upon the temperature of the conduction electrons. In addition, a phenomenological value for the energy relaxation time is estimated from simple considerations of energy balance.

2. THEORY

(a) Free carrier absorption and electron heating

For sufficiently low intensities where two photon processes can be neglected, the absorption of CO₂ laser radiation at wavelengths between 9 and 11 μm ($h\nu = 0.117 \text{ eV}$) in *n*-InSb will take place through interaction with free electrons in the conduction band. Electrons excited to high energies by absorption of a photon may undergo energy relaxation through two competing processes: electron-electron scattering and polar-optical phonon emission. This phonon emission transfers the absorbed energy of the photoexcited electrons to the lattice. Electron-electron scattering, on the other hand,

distributes the absorbed photon energy within the electron gas. If this process is sufficiently fast, i.e. if the concentration is high enough, a non-equilibrium carrier distribution will be established, which is characterized by an electron temperature, T_e . It should be noted that the polar-optical phonons emitted by the photoexcited electrons decay to acoustic phonons through a three phonon interaction and thus have a long lifetime[3]. Some of these optical phonons may therefore be reabsorbed by the electron gas providing an additional source of heating besides the electron-electron thermalization process.

The ultimate transfer of the absorbed photon energy to the environment surrounding the sample takes place through acoustic phonons, either emitted directly by the gas or created (in pairs) by the decay of optical phonons. But since the rate of emission of acoustic phonons is slow compared to that for emission of optical phonons, this will not become a significant energy loss mechanism until the electron gas has cooled below the point where optical phonon emission can take place.

Hearn[4, 5] has made calculations for InSb at liquid helium temperatures which indicate that, for concentrations above a critical value of $n_c = 10^8$ to 10^{11} cm^{-3} , electron-electron scattering should dominate. High magnetic field calculations[6, 7] raise the estimated concentration at which T_e is valid to $n_c \sim 10^{14} \text{ cm}^{-3}$. However, the assumption used in these papers that the Landau levels above the bottom $N=0$ level will not be populated is not valid under the conditions of this experiment. We assume for the electron concentrations of interest here ($n = 1.4 \times 10^{15} \text{ cm}^{-3}$), that the energy distribution of the electron gas with laser heating will be characterized by a temperature, T_e , which is greater than the lattice temperature, T_l . This distribution will then be cooled by a combination of optical and acoustic phonons. The effects caused by emission of optical phonons prior to thermalization of the photoexcited electrons present additional complications.

(b) Shubnikov-de Haas effect under carrier heating conditions

Isaacson and Bridges[8] first used the SdH effect in InSb to obtain hot electron temperatures with applied

†Work supported in part by the Office of Naval Research.

‡On leave from Ludwig Boltzmann Institut fuer Festkoerperphysik and Institut fuer Angewandte Physik, Universitaet Wien, Austria

electric fields. Further electric field induced hot carrier studies were made using the SdH effect by Bäuer and Kahlert [9-11]. In this paper, we show that the SdH effect can also be used to study laser-induced hot electrons. The SdH oscillations in the longitudinal magnetoresistance of a degenerate semiconductor can be observed under the following conditions [12]:

$$\omega_c Y > 1, \hbar\omega_c > k_B T_e, e_F > \hbar\omega_c, \quad (1)$$

where $\omega_c = eB/m^*C$, is the cyclotron resonance frequency and Y is the collision time. Assuming that the Dingle temperature and the spin-splitting factor remain constant as the electron temperature changes, the ratio of SdH amplitudes at two temperatures is given by

$$\frac{A_1}{A_2} = \frac{X_1/\sinh(X_1)}{X_2/\sinh(X_2)} \quad (2)$$

where

$$X_i = 2\pi^2 k_B T_i / \hbar\omega_c \quad (3)$$

The use of eqn (2) to extract the temperature of the hot electron gas is presented in Section 4 of this paper.

(c) Relaxation time

The calculation of a phenomenological relaxation time is based upon the balance of energy gain and loss processes for the electron gas in the illuminated sample volume. The energy gain is due to the absorption of laser photons and subsequent thermalization of photoexcited electrons while the loss is due to energy transfer from the electron gas to the lattice. The energy balance equation for a single electron has the form

$$\frac{d\epsilon}{dt} = -\frac{\epsilon(T_e) - \epsilon(T_l)}{\tau} + P_{abs} \quad (4)$$

where P_{abs} is the absorbed power per electron in the illuminated sample volume and τ is the energy relaxation time. The temperature dependence of the mean energy of an electron in a degenerate semiconductor is taken to be [13]

$$\epsilon(T) = \frac{k_B T F_{1/2}(\eta)}{F_{1/2}(\eta)}, \quad (5)$$

and where

$$\eta = \frac{\epsilon_F}{k_B T}$$

is the reduced Fermi energy.

If a steady-state condition can be established under laser illumination so that

$$\frac{d\epsilon}{dt} = 0, \quad (6)$$

then τ may be calculated from the equation

$$\tau = \frac{\epsilon(T_e) - \epsilon(T_l)}{P_{abs}} \quad (7)$$

The assumption was made earlier that thermalization of the photoexcited electron occurs through electron-electron scattering before significant optical phonon emission from the photoexcited carriers takes place. However, when phonon emission takes place prior to thermalization e.g. to satisfy momentum conservation during photon absorption, a more detailed theoretical treatment would be required.

3. EXPERIMENTAL WORK

The samples used were cut from a bulk sample of *n*-type InSb having a concentration of $1.4 \times 10^{16} \text{ cm}^{-3}$ and a Hall mobility of $12 \times 10^5 \text{ cm}^2/\text{V sec}$ at 1.5 K. The optical surfaces were ground with Al_2O_3 polish with a grit size of $0.3 \mu\text{m}$ ($\sim \lambda/30$). The absorption coefficient at $10.6 \mu\text{m}$ is taken to be 0.032 cm^{-1} which is an extrapolated value taken from Patel [14], who measured 0.3 cm^{-1} for a sample $1.3 \times 10^{16} \text{ cm}^{-3}$. The final sample dimensions were $6.5 \text{ mm} \times 1.8 \text{ mm} \times 0.07 \text{ mm}$ thick. Two current contacts and two potential contacts were made with $25 \mu\text{m}$ diameter gold wire using indium solder.

Figure 1 shows a schematic diagram of the equipment as used in this experiment. The sample was illuminated with a pulse produced by mechanically chopping a beam (TEM₀₀ mode) from a cw CO_2 laser. The pulse width used in this experiment was $\sim 3 \mu\text{sec}$ (F.W.H.M.) with a rise time of $\sim 2 \mu\text{sec}$. The repetition rate was 2000 Hz. The pulse was focussed to a diameter of 1.8 mm at the sample and positioned to illuminate the region of the sample between the potential contacts. The CO_2 laser is grating tuned and produces single line outputs of several watts over most of the $9 \mu\text{m}$ to $11 \mu\text{m}$ wavelength range. The experiment reported here was carried out at $\lambda = 10.3 \mu\text{m}$ with powers up to 10 watts available. A He-Ne laser used in conjunction with a silicon PIN photodiode produced a trigger pulse for the pulse generating and delaying electronics.

The magnetoresistance of the sample was then measured using a short (5 nsec) electrical probe pulse generated by a fast rise time ($< 1 \text{ nsec}$) Tektronix pulse generator. The electrical pulse, kept small to avoid heating by the electric field, was synchronized to coincide with the peak of the laser pulse. The difference voltage between the two potential probes was measured with a Tektronix 7904/7S14 sampling oscilloscope.

Previous pulsed d.c. SdH measurements [15] reported by the authors were made by directly recording the output of the sampling oscilloscope vs. magnetic field. However, significant improvements in signal-to-noise ratio have been obtained through the use of magnetic field modulation in combination with the fast sampling methods. This combined technique was first developed by Kahlert and Seiler [16, 17] for observing hot electron magnetophonon structure in *n*-InSb at 77 K. When used to observe the SdH effect, this technique produces a detector response which is proportional to the first derivative of the magnetoresistance oscillations, but it does not affect the ratio of amplitudes as given in equation (2). In this method, the output of the sampling oscilloscope is fed into a lock-in amplifier, the output of which is then recorded.

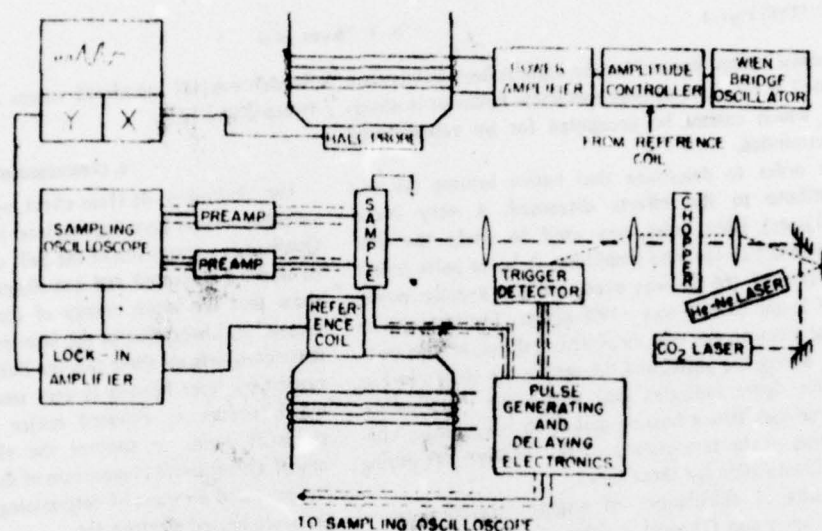


Fig. 1. Block diagram of experimental apparatus

4. RESULTS AND ANALYSIS

Figure 2 shows SDH oscillations for lattice temperatures, T_l , between 1.8 and 9.6 K. The oscillations recorded for various incident laser powers are shown in Fig. 3 for $T_l = 1.8$ K. Qualitatively, it can be seen that the oscillations are damped by increasing laser power in a manner analogous to the damping caused by elevated lattice temperatures. These data show directly that the mean energy of the electron gas increases with laser illumination.

The SdH amplitude ratios as a function of lattice temperature (without laser illumination) are plotted on the left-hand side of Fig. 4 and exhibit the characteristic dependence given by eqn (2). The variation of the amplitude ratio with incident laser power is plotted on the right-hand side of Fig. 4. The reference amplitude A_0 for both graphs was taken at 1.8 K with no laser illumination.

The electron temperature corresponding to each laser power is determined by comparison of the amplitude ratio shown in both halves of Fig. 4. For example, the dotted lines show that, for a 0.98 W peak incident laser

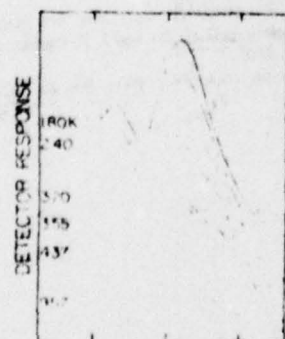


Fig. 2. SdH oscillatory magnetoresistance for several lattice temperatures taken while detecting at the first harmonic of the modulation frequency (no laser illumination).

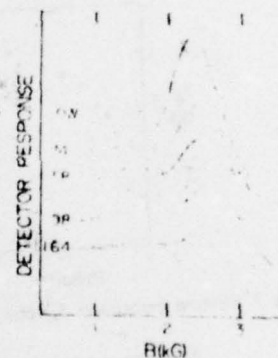


Fig. 3. SdH oscillations for various incident laser powers at a constant lattice temperature of 1.8 K. Power levels listed are peak incident power at the sample.

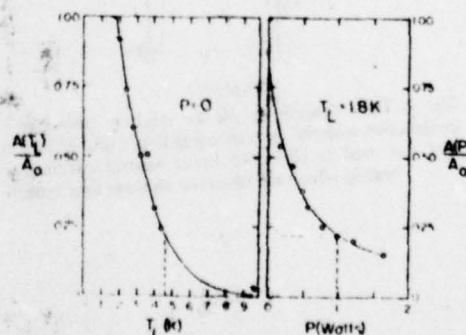


Fig. 4. SdH amplitude ratios versus lattice temp (left) and versus incident laser power (right).

power, an amplitude ratio of 0.22 was obtained. From the temperature dependence it is seen that an amplitude of 0.22 corresponds to a temperature of 4.6 K. Thus, a phenomenological electron gas temperature of 4.6 K is obtained for an incident laser power of 0.98 watts at a lattice temperature of 1.8 K. The electron temperatures

obtained in this manner for the various laser powers are plotted in Fig. 5. A distinct non-linear behavior is observed which cannot be accounted for by experimental uncertainties.

In order to determine that lattice heating did not contribute to the effects discussed, a very broad ($\sim 30 \mu\text{sec}$) laser pulse was used to study the time dependence of the SdH amplitude. A lower pulse repetition rate of 166 Hz was used, but the average power input to the sample was $\sim 50\%$ higher. The temperature of the electron gas was measured at different time positions during the pulse, and the results are shown in Fig. 6. This figure indicates that within the experimental uncertainties lattice heating makes an insignificant contribution to the temperature of the electron gas during laser illumination for these times.

Results of calculations of energy relaxation times based upon eqn (7) yield a value of about 25 nsec for electron temperatures between 3.2 and 5.2 K.

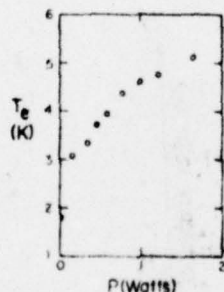


Fig. 5. Electron temperature T_e versus laser power.

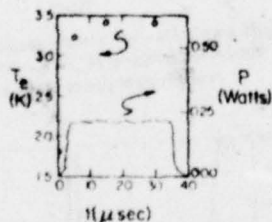


Fig. 6. Time dependence of the electron temperature T_e in conjunction with the corresponding laser pulse of long duration that was used to check for lattice heating effects. No lattice heating effects are observed on these time scales.

Sandercock [18] calculated values of $1/\tau \sim 10^7 \text{ sec}^{-1}$ between 2 and 12 K.

5. CONCLUSIONS

The Shubnikov-de Haas effect has been shown to be a valuable tool for investigating laser induced hot electrons. Qualitative comparison of the SdH oscillations as recorded under illuminated and non-illuminated circumstances show that the mean energy of the electron gas is increased by absorption of the laser radiation. In addition, these comparisons show that the SdH amplitude damping caused by laser heating is very similar to the damping which occurs at elevated lattice temperatures. This similarity tends to support the electron temperature model. Quantitative comparison of these amplitude ratios has provided a means of determining the temperature of the laser heated electron gas.

On the basis of the electron temperatures derived from these measurements, a phenomenological energy relaxation time has been determined. Further experiments are planned which should provide additional insight into the physical nature of this relaxation process.

REFERENCES

1. B. V. Rollin, *Phys. Soc. Proc.* **77**, 1102 (1961).
2. Sh. M. Kogan, *Sov. Phys.-Solid State* **4**, 1386 (1963).
3. D. K. Perry, *Phys. Rev.* **B8**, 1544 (1973).
4. C. J. Hearn, *Proc. Phys. Soc.* **B6**, 881 (1965).
5. C. J. Hearn, *Phys. Lett.* **20**, 113 (1966).
6. A. M. Zlobin and P. S. Zyryanov, *Sov. Phys.-Uspekhi* **14**, 379 (1972).
7. Sh. M. Kogan, V. D. Shadrin and A. Ya. Shulman, *Sov. Phys.-Jett.* **41**, 686 (1975).
8. R. A. Isaacson and F. Bridges, *Solid State Comm.* **4**, 635 (1966).
9. G. Bauer and H. Kahlert, *J. Phys. C* **6**, 1253 (1973).
10. H. Kahlert and G. Bauer, *Phys. Rev.* **B7**, 2670 (1973).
11. G. Bauer and H. Kahlert, *Phys. Rev.* **B5**, 566 (1972).
12. P. N. Argyres, *J. Phys. Chem. Solids* **4**, 19 (1959).
13. G. Bauer in *Springer Tracts in Modern Physics*, Vol. 74, p. 1. (Springer-Verlag, New York (1974)).
14. C. K. N. Patel and E. D. Shaw, *Phys. Rev.* **B3**, 1279 (1971).
15. B. Moore, D. G. Seiler, and H. Kahlert, *Bull. Amer. Phys. Soc.* **22**, 460 (1977).
16. H. Kahlert and D. G. Seiler, *Rev. Sci. Instr.*, To be published.
17. H. Kahlert, D. G. Seiler and J. R. Barker, *Solid-St. Electron. Ms No. 770*.
18. J. R. Sandercock, *Proc. Phys. Soc.* **B6**, 1221 (1965).

VI. FUTURE PLANS

A. Experimental

1. Lasers

A Lansing Piezo-Electric Translator will be used to better control the mode patterns in the cw lasers, along with an increase in power and possibly more stability.

For the CO laser, a better grating rotation system is almost completed and will be installed. In addition, a Bausch and Lomb grating with >92% efficiency will be utilized. Consequently, the power and the number of observed laser lines should increase. An improved laser tube will be constructed that has an integral gas ballast chamber which should increase the operational lifetime of the laser.

Q-switching with a rotating mirror will also be developed this year.

2. Installation of Electro-Optic Switch

An electro-optic switch composed of a high quality CdTe crystal has been ordered and will be installed. Driven by a high power voltage generator with fast electrical rise and fall times it will then enable short laser pulses to be produced. We are in the process of ordering a Velonex generator which will enable pulses as short as 50 nsec to be obtained. The power supply has the versatility to be able to supply variable pulse lengths and repetition rates.

3. Extension of CO₂ Laser-Induced Hot Electron Measurements to Higher Carrier Concentrations

Up to the present time, only one concentration ($\approx 1 \times 10^{15} \text{ cm}^{-3}$) sample of n-InSb has been investigated by SdH measurements under laser irradiation. Higher concentration samples of n-InSb will be investigated this coming year. Since free carrier absorption depends directly upon the number of free carriers, some interesting laser-induced hot electron properties may emerge.

4. Measurements of CO Laser-Induced Hot Electrons

The development of a CO laser in our laboratory will enable us to determine the effect of CO laser radiation on InSb. The CO laser has about twice the photon energy of the CO₂ laser and consequently should produce some interesting hot electron effects.

B. THEORETICAL

This coming year a major effort will be made to analyze and understand the laser-induced heating effects that have been observed. The models that are developed will have to take into account free carrier absorption and energy loss rates. A qualitative overview of many of the processes involved is given in Fig. 15 where a block diagram is presented.

The free carrier absorption process can take place with emission of optical phonons and/or acoustic phonons. In addition, ionized impurity scattering may have to be taken into account. Thus this absorption process creates photoexcited electrons at energies high in the conduction band. Assuming that electron-electron scattering predominates over optical phonon emission, the electron distribution will then relax to a quasi-equilibrium distribution characterized by an electron temperature of the heated electron gas. There are indications that this is a valid assumption, but confirming theoretical work needs to be done.

Energy-loss rates of the hot electron gas to the lattice must be investigated. Since the electron temperature of the gas under laser radiation is never very large, optical phonon emission can probably be neglected. The predominate energy-loss rate is undoubtedly due to the acoustic modes via deformation potential and piezoelectric coupling. The relative importance of piezoelectric scattering compared with deformation-potential scattering depends upon carrier concentration. Consequently, at low electron concentrations piezoelectric scattering will predominate, whereas at high electron concentrations deformation

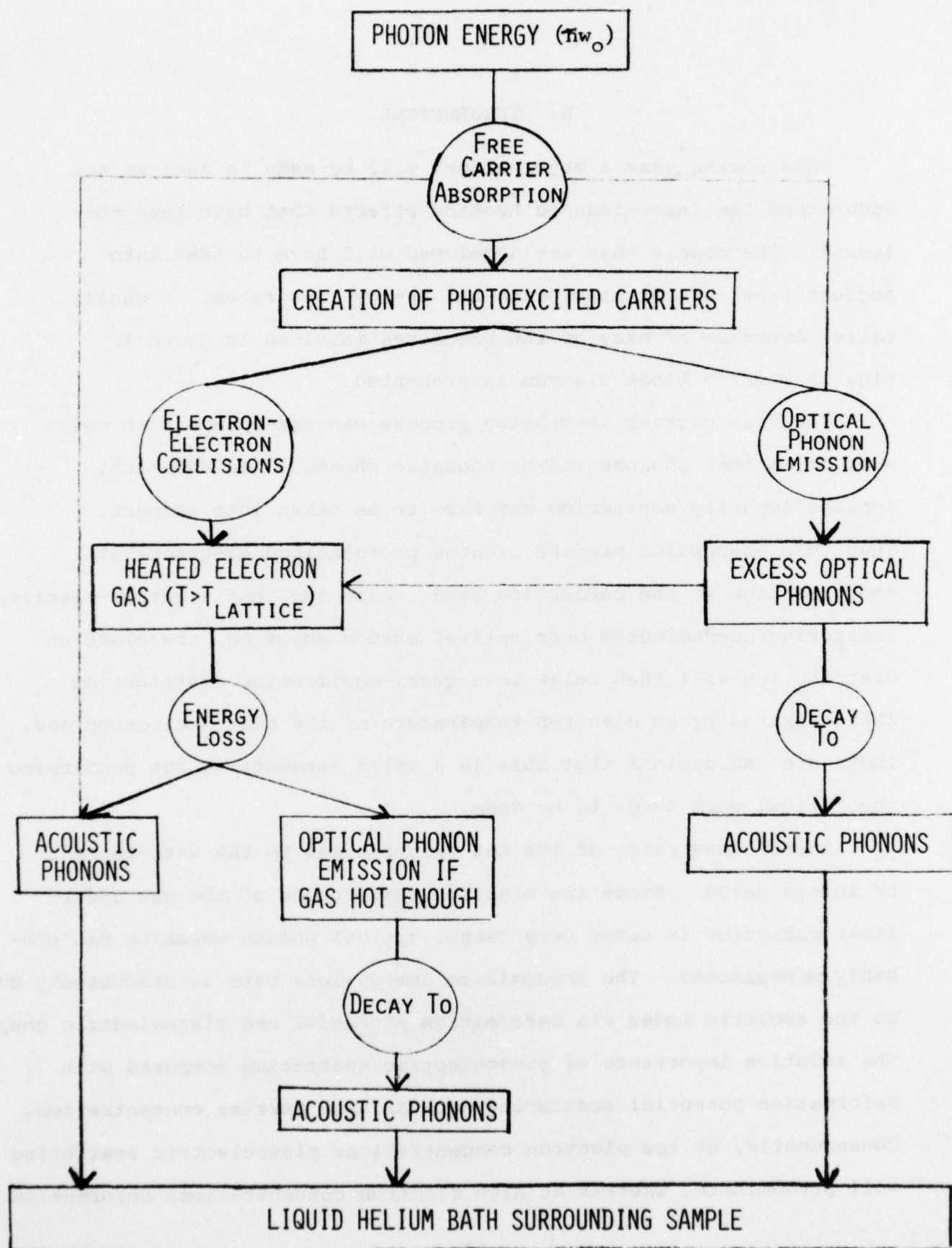


Figure 15. Block diagram of some absorption and scattering processes involved in laser-induced heating of the electron gas.

potential scattering will predominate.

We have enlisted the aid of two theoreticians for the study. Dr. Donald Kobe is a professor at NTSU and has a background in statistical mechanics and the many-body problem. Recently, he has turned his attention to understanding the nature of the interaction of laser radiation with matter. He is certainly familiar with most of the theoretical machinery necessary to handle this problem.

Dr. J. R. Barker, University of Warwick, England, will be visiting our university, January through May, 1978, as a visiting professor. He is intimately acquainted with quantum transport theory and in particular hot electrons. Consequently, he brings some needed expertise to the project just at the time when it is needed.

VII. TECHNICAL PERSONNEL

Research Associate

Dr. H. Kahlert of the Ludwig Boltzmann Institut fur Festkorperphysik in Vienna, Austria, worked with this project from October 1, 1976 through September 5, 1977. Both his experimental and theoretical expertise in the area of hot electrons in semiconductors were utilized.

Graduate Students

The following graduate students have worked on various aspects of this project:

Mr. Delbert Dowdy

Mr. Mike Goodwin

Mr. Larry Hanes

Mr. Brad Moore

Mr. Larry Tipton

VIII. REPORT ON

The International Conference on Hot Electrons in Semiconductors was held on the campus of North Texas State University, Denton, Texas, 6-8 July 1977. There were over 130 participants from 13 countries. This Conference was a Topical Conference of the American Physical Society and abstracts were published in the Bulletin of the American Physical Society, Series II, Vol. 22, No. 6, June 1977. Other sponsors were the Office of Naval Research and North Texas State University, in cooperation with the Electron Device Society of IEEE and the U.S. Army Research Office.

The purpose of the Conference was to bring together scientists interested in all aspects of hot or non-equilibrium carriers in semiconductors. Topics of current interest and importance were presented and discussed with particular emphasis on bulk transport, surface and interface transport, device behavior and photo-excitation. A final session of the conference was devoted to a discussion of unsolved problems which deserve future theoretical and experimental effort.

Much "hot electron" work has traditionally been presented at the International Conferences on the Physics of Semiconductors. Prior to this Conference, an International Symposium on High Field Transport in Semiconductors was held in Modena, Italy, 4-6 July 1973. In addition, many papers given at the Symposium on Instabilities in Semiconductors 20 and 21 March 1969 at the Thomas J. Watson Research Center in Yorktown Heights, N.Y. (see the IBM Journal of Research and Development, Vol. 13, No. 5, September 1969) were devoted to hot electron effects.

The following individuals handled the organizational and program aspects of the conference:

Conference Chairman

Dr. D.G. Seiler
Department of Physics
North Texas State University
Denton, Texas 76203

Conference Vice-Chairmen

Drs. A.L. Smirl & J.R. Sybert
Department of Physics
North Texas State University
Denton, Texas 76203

Program Committee

Dr. J.R. Barker
Department of Physics
University of Warwick
Coventry, U.K.

Dr. H. Kahlert
Ludwig Boltzmann Institut Für Festkörperphysik
Kopernikusgasse 15
A-1060 Vienna, Austria

Dr. M.A. Littlejohn
Department of Electrical Engineering
North Carolina State University
Raleigh, North Carolina 27607

Dr. M.O. Scully
Optical Sciences Center
University of Arizona
Tucson, Arizona 85721

Dr. R.E. Leheny
Bell Telephone Laboratories
Holmdel, New Jersey 07733

Dr. D.K. Ferry
Office of Naval Research
Arlington, Virginia 22217

Dr. A.B. Fowler
IBM Watson Research Center
Yorktown Heights, New York 10598

Dr. H. Heinrich
Institut Für Physik
Johannes Kepler University
A-4045 Linz, Austria

Dr. J. Holm-Kennedy
Department of Electrical Engineering
University of Hawaii
Honolulu, Hawaii 96822

The following pages contain a copy of the abstracts of the conference as published in the Bulletin of the American Physical Society, Series II, Vol. 22, No. 6, June 1977, pp. 700-711. Next, a list of the conference attendees is given.

INTERNATIONAL CONFERENCE ON HOT ELECTRONS IN SEMICONDUCTORS

Denton, Texas
6-8 July 1977

PREAMBLE

An International Conference on Hot Electrons in Semiconductors will be held on the campus of North Texas State University in Denton, Tex. on 6-8 July 1977. The purpose of the conference is to bring together scientists interested in all aspects of hot or nonequilibrium carriers in semiconductors. All persons interested in this field are welcome.

The conference is sponsored by the Office of Naval Research, the American Physical Society, and North Texas State University in cooperation with the Electron Device Society of IEEE and the U.S. Army Research Office.

The program is arranged into six sessions of 17 invited papers and 42 contributed papers. Extended discussion time has been allotted for all papers. In addition, a rump session on Saturday morning will be devoted to an open discussion on future trends in the area of hot electrons.

Registration will begin Tuesday evening at 6:00 P.M. in conjunction with a reception in Maple Hall. The fee for the conference will entitle the participant to attend the conference banquet and the social hours and to receive a copy of the proceedings. Advanced registration fee (must be received by chairman by 1 July 1977) is \$40.00. Registration fee after 1 July 1977 is \$45.00. Make checks (U.S. dollars only) payable to North Texas State University, Account 77983.

Students are not required to pay the conference fee. Copies of the proceedings and a limited number of banquet tickets will be available for purchase on 6 July.

Members of the program committee are J.R. Barker, University of Warwick; H. Kahlert, currently at North Texas State University; M.A. Littlejohn, North Carolina State University; M.O. Scully, University of Arizona; R.F. Leheny, Bell Telephone Laboratories; K.D. Ferry, Office of Naval Research; A.B. Fowler, IBM Watson Research Center; H. Heinrich, Johannes Kepler University; J. Holm-Kennedy, University of Hawaii. The conference is being organized locally by D.G. Seiler, A.L. Smirl, and J.R. Sybert.

Detailed information is available for those planning to come to the conference. Please write the conference chairman, Dr. David G. Seiler, Department of Physics, North Texas State University, Denton, Tex. 76203. [Telephone: (817) 788-2626.]

EPITOME

(All the technical sessions will be held in the Golden Eagle Suite of the North Texas State University Union Building. There will be coffee breaks each morning and afternoon. Personal names are those of invited speakers.)

WEDNESDAY MORNING

- 8:30 Welcome: Seiler, Sybert, C.C. Nolen (President of North Texas State University).
8:45 A General Session: Hilsum, Price, Bauer, Shah, Ulbrich.

WEDNESDAY AFTERNOON

- 2:00 B Devices and Bulk Transport: Kroemer.

THURSDAY MORNING

- 9:00 C Mostly MOSFET's: Ferry, Hess.

THURSDAY AFTERNOON

- 1:30 D Optically Excited: Auston, Scully, Hearn, Leite, Weisbuch.

FRIDAY MORNING

- 9:00 E Quantum Transport: Barker.

FRIDAY AFTERNOON

- 1:30 F Mainly Bulk Transport: Hughes, Thornber, Ning.

SATURDAY MORNING

- 9:00 G Rump Session on Future Trends.

MAIN TEXT

WELCOME

Wednesday morning, 6 July 1977; Golden Eagle Suite at 8:30 A.M.; D.G. Seiler, presiding

SESSION A: GENERAL

Wednesday morning, 6 July 1977; Golden Eagle Suite at 8:45 A.M.; E. Conwell, presiding

Invited Papers

A 1. Historical Background of Hot Electron Physics. C. HILSUM, *Royal Radar Establishment, England*. (30 min.)

A 2. Techniques of Calculation of Hot Electron Phenomena. P.J. PRICE, *IBM, Thomas J. Watson Research Center*. (30 min.)

Analytical formulas are generally able to give a better account of a physical phenomenon than can be provided by a numerical description. The latter may be necessary for hot electrons, however, because of the inability of simple physical principles (such as relaxation times) to truly encompass the dynamics of the distribution function, and because of complexity in the band and scattering scheme of the solid, of the particular phenomenon studied, or geometry of the situation. The traditional phenomenon of interest is the steady state with spatial homogeneity, and independent non-degenerate electrons. In suitable conditions the Boltzmann equation then reduces to one in a single variable (energy) which can be solved by relatively simple means. More generally, for this case, we need a computation of the distribution function. Either the latter is represented by its values on a grid of points in the space of the electron variables, and the operators of the Boltzmann equation by operations on this array, or the "history" of a single electron is simulated by a Monte Carlo scheme. The former method has advantages within its range of applicability. Monte Carlo has been extensively applied, because of its greater ability to deal with band and scattering details; it is also applicable, by elaboration of the computational procedures, to a wider range of phenomena of interest. Following a description of basic methods and their applications, the needed extensions of method will be discussed with application to phenomena such as time dependence; diffusion; impact ionization; effects of carrier-carrier interaction; field-effect surface scattering; thermalization of drifting carriers; semiconductor junctions; effect of degeneracy. Some particular calculations will be used for illustration.

A 3. Experimental Aspects of Hot Electron Distribution Functions.

G. BAUER, *Physikalisches Institut, RWTH Aachen, Germany*. (30 min.)

The experimental determination of hot carrier distribution functions has been of steady interest since the early days of hot electron transport investigations. A motivation for performing these studies was the hope to get direct experimental evidence for the various scattering mechanisms from the shape of the distribution function. This rather fundamental experimental information should, in principle, be more appropriate for a comparison with theoretical predictions than transport properties of hot carriers alone. In this paper a review will be presented on the experimental efforts to obtain high field distribution functions in bulk materials. Three optical methods will be discussed in detail: (i) inter- and intraband absorption measurements, (ii) emission due to radiative transitions between band states, and band- and impurity states, (iii) inelastic light scattering experiments. A distinction is made between methods which yield the energy distribution function and those which give information on the anisotropic distribution of hot carriers in the momentum space. The latter experiments involve a determination of the electric field induced dichroism in absorption or emission and the dependence of the scattering cross section on scattering geometry in inelastic light scattering experiments. The influence of the non-equilibrium phonon distribution on the interpretation of the experimental results is discussed, too. In addition, current work on energy distribution functions of hot carriers in quantizing magnetic fields as obtained from absorption or emission of infrared radiation due to transitions of carriers between Landau states or magnetic field split impurity states will be presented.

* Supported in part by the Deutsche Forschungsgemeinschaft.

** Present address: Experimentelle Physik IV, Universität Ulm, Germany.

Contributed Papers

A4. Experimental and Theoretical Determination of Hot Electron Distribution in GaAs and Related Mixed Crystals, M. INOUE, N. TAKENAKA, J. SHIRAFUJI, and Y. INUISHI, *Osaka U.* -- The experimental attempt to

investigate the non-Maxwellian electron distribution was made on the basis of the field-dependent photoluminescence spectrum and the result was elaborately compared with Monte Carlo calculation including all possible scattering mechanisms. The photoluminescence spectrum due to band-to-band or band-to-acceptor transition in GaAs, GaAsP and AlGaAs was measured under high electric fields.¹ In mixed crystal with a small energy separation between Γ and X valleys, a peculiar electron distribution resulting from dominant intervalley scattering of hot electrons was

observed at relatively lower electric fields than in GaAs.

¹M. Inoue, N. Takenaka, J. Shirafuji, and Y. Inuishi, *Proc. Intern. Conf. Phys. of Semicond.* (1976)

A5. Carrier Distribution Function for Warm Electrons.

S. ZUKOTYNSKI and W. HOWLETT, *University of Toronto*. -- The principal of equal a-priori probabilities is used to deduce some of the general properties of the distribution function in the presence of external fields. A trial function for the transport equation is constructed and a closed form solution is found that is applicable in the warm electron range. A comparison with experimental data for drift velocity in germanium and in silicon gives excellent agreement in the warm electron range. *Supported by National Research Council of Canada.

Invited Papers

A 6. Hot Electrons and Phonons under High Intensity Photoexcitation of Semiconductors.
JAGDEEP SHAH, *Bell Telephone Laboratories, Holmdel. (30 min.)*

It has become well established during the last few years that intense photoexcitation of a semiconductor with photons of energy larger than the bandgap energy leads to the heating of the photoexcited carriers and the generation of nonequilibrium phonons. These phenomena result from the relaxation of photoexcited carriers to the band minimum or maximum by interaction with other carriers and by emission of phonons. At relatively low intensities ($< 10^5 \text{ W/cm}^2$ for GaAs) the photoexcited carrier distribution is Maxwellian with a carrier temperature T_c different from the lattice temperature. T_c as high as 150 K and phonon temperatures as high as 900 K have been observed in GaAs. The observed variation of T_c with excitation intensity leads to the conclusion that in semiconductors like GaAs the polar optical mode scattering is the dominant energy loss mechanism from the electron gas to the lattice. The understanding achieved through such experiments in GaAs and CdSe enables us to predict with reasonable confidence the carrier temperatures in semiconductors in which polar optical mode scattering dominates. At higher intensities ($> 10^5 \text{ W/cm}^2$ for GaAs), the carrier distribution becomes non-Maxwellian for reasons not well understood at present. We will also discuss some recent measurements of variation of T_c with excitation wavelength and of the transmission spectra of photoexcited GaAs. We will also consider the implications of carrier heating in interpreting other high intensity experiments.

A 7. Experimental and Theoretical Low Intensity Photoexcitation Phenomena.
R.G. ULBRICH, *Institut für Physik, Universität Dortmund, Federal Republic of Germany. (30 min.)*

High-resolution emission spectroscopy of band-to-impurity optical transitions in GaAs is used to measure the energy distribution functions $f(E)$ of electrons and holes in optically excited carrier plasmas at well defined, low densities ($10^9 \text{ cm}^{-3} \leq n \leq 10^{13} \text{ cm}^{-3}$). With this experimental method we probe (i) the energy relaxation of initially hot carrier distributions after pulsed photoexcitation ($\hbar\omega \gg E_g$), (ii) stationary non-equilibrium distributions of electrons in the conduction band under cw photoexcitation ($\hbar\omega \geq E_g$) and (iii) the transport properties of photoexcited carrier plasmas in low electric fields ($0 \leq |E| \leq 20 \text{ V/cm}$). The observed distribution functions are compared with theoretical results on the basis of the known band structure data of GaAs, taking into account polar optic and acoustic phonon scattering, the interaction among the carriers, ionized impurity scattering, and using approximate solutions of the appropriate transport equation.

Contributed Paper

A8. Non-Equilibrium Distribution Function of Carriers in Semiconductors, WAFIK A. WASSEF--A General Form of the carrier distribution function in semiconductors in the presence of an external electric field and a steady flow of carriers is presented. It is shown that this distribution function reduces to some well known forms under certain simplified conditions. Some of the implications concerning the ergodic hypothesis, the free energy and entropy are discussed. The scattering mechanisms are taken

into consideration in two different approaches: 1. a phenomenological approach in which we require that the average mobility of carriers for a given field is maximum. This criterion is shown to reduce to the well known principle of minimum free energy and consequently maximum entropy at thermal equilibrium. 2. a specific scattering mechanism is considered in setting up the energy balance equation. The skewness and cut-off value of the deduced distribution function are given direct physical interpretations. The variation of mobility with temperature is presented and is found to agree with experimental result fairly well.

SESSION B: DEVICES AND BULK TRANSPORT

Wednesday afternoon, 8 July 1977; Golden Eagle Suite at 2:00 P.M.; R. Bets, presiding

Invited Paper

B 1. Review of Theoretical and Experimental Aspects of Hot Electrons in Devices.
H. KROEMER, *Department of Electrical Engineering and Computer Science, University of California, Santa Barbara. (30 min.)*

Much of the early research on hot electron effects in devices utilized a quasi-static local model in which the local carrier drift velocity was assumed to be an instantaneous function of the local electric field. The point of diminishing return for such models has been reached, and recent work has stressed non-local, non-instantaneous dynamics effects. For example, the electrons in GaAs and InP cannot scatter into the satellite valleys until they have acquired the necessary energy, which requires both space and time. The spatial consequences lead to drastic drift velocity overshoots, which improve the performance of FET's but degrade that of TE devices. The static negative differential conductance of the latter is also influenced. The temporal consequences govern the ultimate fre-

quency limits, particularly of TE devices. The higher the fields, the higher the speed. Hence LSA operation is not the fastest operation, and InP is faster than GaAs. Hypothetical superlattice negative conductance does not offer the speed advantage often claimed. The dynamics effects depend on the strength of the intervalley scattering, and on the forward-scattering nature of polar scattering in III-V compounds. At high fields the two effects combine to a less random electron dynamics than if the high electron energy were purely thermal, leading to noise reduction, and simplifying the electron dynamics, giving good qualitative insights without much mathematics. For a quantitative analysis, several numerical techniques have been developed. Displaced-Maxwellian techniques are reasonably simple and give a good qualitative account of the deviations from quasi-static models, but are incapable of modeling quantitatively the effects of the sharp energy threshold of strong intervalley scattering. Perhaps the best technique is Rees' modeling of the actual distribution function by time-dependent superposition of a carefully chosen set of ad-hoc functions.

Contributed Papers

B2. Hot Electron Transport Effects in Field Effect Transistors (FET). *H.L. GRUBIN and T.M. MCHUGH, United Technologies Res. Cen.--Present semiconductor devices may be placed in one of two groups according to whether hot electron effects are or are not responsible for their operation. Gunn oscillators fall into the former category whereas FET devices are in the latter. Currently used FET materials such as GaAs are, however, subject to electron transfer with significant negative differential mobility and device operation may be expected to reflect this contribution. We have developed a program that numerically simulates the space and time dependent effects of negative differential mobility on FET operation. We will illustrate: (1) the transient formation of high field domains within the conducting channel and conditions necessary for propagation and recycling between the gate and drain contacts; (2) stationary space charge configurations specific to the presence of negative differential mobility; and (3) the influence of negative differential mobility on the FET response times. *Supported by the Office of Naval Research.

B3. Transferred Electron Effects in n-GaAs and n-InP Under Hydrostatic Pressure. *W. Czubytyj, M.S. Shur and M.P. Shaw, Wayne State U.--Experimental results will be presented showing the variation of the peak velocity, peak electric field and saturated velocity of the velocity-field curve for n-GaAs under hydrostatic pressure. Similar data will be presented for the field at peak velocity for n-InP. The extraction of the data from the current-voltage characteristics is based on an exploitation of the influence of the boundary conditions on the manifestation of transferred-electron induced (Gunn) current instabilities. Our results, which differ somewhat from those of Vinson et al.¹, will be compared with our Monte Carlo calculations of the velocity-field curves for these materials. This comparison should allow us to verify important conduction-band parameters such as the energies and effective masses of subsidiary minima and the coupling constants for intervalley scattering. *Supported by ONR under contract N-0014-75-C0399 1P.J. Vinson, C. Pickering, A.R. Adams, W. Fawcett and G.D. Pitt, Proc. 13th Int. Conf. Semicon., Rome (1976).

B4. High-Field Properties of n-InP under High Pressure. *T. Kobayashi, **K. Takahara, T. Kimura, K. Yamamoto and K. Abe, Kobe Univ., Japan--The high electric field properties of n-InP at 300 K have been studied as a function of pressure. Hydrostatic measurements are made in the piston and cylinder apparatus, using liquid pressure-transmitting medium. The threshold fields (E_t) for transferred electron instabilities range from 7.5 kV/cm to 8.5 kV/cm at atmospheric pressure. The resistivity of the samples increases with increasing pressure. The most reliable results show that E_t is slightly increased, but is not sensitive to pressure below 40 kbar. These behaviours can be explained qualitatively in terms of possible band structure changes and pressure effects on the electrical contacts. By using known variations of parameters such as effective mass and sub-band energy gaps, detailed theoretical calculations are carried out to fit the data and to confirm the correct model of operation (two- or

three-level operations). Their results were also compared with analogous experiments on GaAs.

*Submitted by K. Yamamoto.

**Supported in part by the Grant-in-Aid for Scientific Research from the Ministry of Education.

B5. Pressure & Composition Dependence of High Field Instabilities in $\text{InAs}_{1-x}\text{P}_x$ Alloys. A.EI-SABBARY and A.R. ADAMS, University of Surrey, UK, and M.L. YOUNG, R.S.R.E., Baldock, UK. -- Experimental and theoretical studies have been made of electron transport and hot electron effects in $\text{InAs}_{1-x}\text{P}_x$ as a function of alloy composition and hydrostatic pressure. Pulsed I-V measurements were made on M shaped samples to determine the threshold field, E_t , and the current, I_t , for the onset of high field instabilities. These were compared with Monte Carlo calculations of the velocity field characteristics. At atmospheric pressure and $x < 0.3$ the high field instabilities were caused by avalanche multiplication and at $x > 0.3$ by Gunn effect and E_t increased steadily with x from 0.9 kV/cm in InAs to ~9 kV/cm in InP. For samples with $x < 0.3$ a pressure of 1 kbar produced an increase in E_t similar to a 1% increase in x , while for $x > 0.3$, E_t remained constant or even decreased with increasing pressure. These variations of E_t in the Gunn regime are in agreement with the theoretical calculations. To try to determine absolute values for the peak velocity from I_t , detailed studies were made of the Hall effect as a function of x , pressure, temperature and magnetic field. The results and calculations give information about the alloy's usefulness for Field Effect Transistors.

B6. Hot Electron- and Magneto-Transport Properties of GaInAsP Liquid Phase Epitaxial Layers. B. B. Houston, J. B. Restorff, J. R. Burke, NSWC White Oak, Md; G. A. Antypas, Varian Associates, Palo Alto, CA; D. K. Ferry, Office of Naval Research, Arlington, VA.-- v-E curves at 77 & 293 K, μ -E curves from 4.2 to 293 K, and magneto-resistance from 4.2 to 293 K in fields to 8 T have been measured on three samples. The samples were lattice matched to (111)B semi-insulating InP substrates. The following table summarizes some of the results:

E_{gap}	$n(77 \text{ K}) \times 10^{-15}$	$\mu(77 \text{ K})$	$v_{sd}(77 \text{ K}) \times 10^{-7}$
eV	cm^3	$\text{cm}^2/\text{V-sec}$	cm/sec
1.05	6.1	19300	3.6
1.2	11.	11000	2.0
1.25	42.	6200	1.6

The mobilities μ and "saturated" drift velocities v_{sd} are lower than expected.¹ The only oscillatory magnetoresistance observed was Shubnikov-de Haas in the sample with the largest n , from which an effective mass can be computed.

*Supported by the NSWC IR Fund and ONR.

¹M. A. Littlejohn, J. R. Hauser and T. H. Glisson, Appl. Phys. Lett. 30, 242 (1977).

B7. Negative Resistance and Peak Velocity in the Central (000) Valley of III-V Semiconductors. J. R. HAUSER, T. H. GLISSON and M. A. LITTLEJOHN, N. C. State U.--It is generally recognized that negative resistance and peak velocity of III-V semiconductors arise from the transfer of electrons at large fields

from the central (000) valley to higher lying minima in the conduction band. This model leads to predictions that higher peak velocities can be achieved in materials in which the energy separation between the central valley and higher minima is as large as possible. One ternary material which appears favorable on this basis is $\text{Al}_{1-x}\text{In}_x\text{As}$ with $x \approx 0.75$ since the separation is around 1 eV with a predicted low field mobility of 11,000 $\text{cm}^2/\text{V}\cdot\text{sec}$. However Monte Carlo high field transport calculations have not resulted in the expected large peak velocity for this material. The peak velocity has been found to be limited by fundamental processes occurring within the central valley. These effects appear to be related to non-parabolicity and give rise to a peak velocity and a negative resistance region for carriers in only the central valley without high field transfer to higher lying minima. These central valley limits have also been calculated for GaAs by confining carriers to the central valley. However for GaAs the transfer of carriers to the upper valley is found to occur before these fundamental central valley limits occur.

*Supported by the Office of Naval Research, Wash., D.C.

B8. Travelling Dipole Domains and Fluctuations for a Current Instability Due to Bragg-Scattering¹. M. BUETIKER, M. THOMAS, University Basel. --We investigate the stability of uniform and nonuniform current states for a model in which Bragg-scattering of hot electrons leads to bulk negative differential conductivity. The system is described by phenomenological balance equations for momentum and energy densities of the carriers¹. For fixed total current, we find a family of periodic travelling-wave solutions which are unstable against a continuum of modes, and a solitary solution (dipole domain) which can be stabilized by coupling to a suitable external circuit, if the static domain impedance is negative. The model describes therefore a discontinuous nonequilibrium phase transition to a large-amplitude domain. In order to study fluctuations, we add stochastic forces to the balance equations and discuss the resulting fluctuation spectra.

*Supported by the Swiss National Science Foundation
M. Buttiker, M. Thomas, Phys. Rev. Lett. **38**, 78 (1977)

B9. High Field Transport in PbTe. W. JANTSCH, J. ROZENBERG, H. HEINRICH, Johannes Kepler Universität. --The drift velocity and Hall coefficient of n- and p-type PbTe at 77K were measured for various crystallographic directions of current up to field strengths of 1.5 kV/cm. Both the conductivity and the Hall effect are anisotropic and the latter depends also strongly

on the magnetic field. These effects are attributed to nonuniform heating of the equivalent conduction band F- valleys of PbTe and equivalent intervalley transfer. For field strengths beyond 1 kV/cm oscillations of the current and the potential distribution occur. The Hall coefficient decreases sharply above this threshold indicating avalanche breakdown. Probing the potential distribution, it could be shown, that this instability is caused by high field domains, which travel down the sample with the drift velocity of the carriers. Possible mechanisms for the formation of high field domains are discussed.

B10. Hot Carriers in Lead Chalcogenides. P.M. TOMCHUK, V.A. SHENDEROVSKIY, Institute for Physics, Ukr. Academy of Sciences, Kiev. --Effect of the heating electric field on galvanomagnetic coefficients of lead chalcogenides is treated theoretically with account for the complicated shape of constant-energy surfaces and the anisotropy of scattering mechanisms. The calculations are carried out on the basis of the approximations which were shown realistic for the substances within considered range of temperatures and field intensities¹. Characteristic property of hot carriers behaviour is shown to distinguish lead chalcogenides from Ge, Si or A_3B_5 semiconductors. Anisotropy of the energy dispersion essentially affects both the carriers distribution function, due to the dependence of the electronic temperature on the anisotropy parameter, and the values of the kinetic coefficients.
¹P.M. Tomchuk, V.A. Shenderovskij, Ukr. Fiz. Zh. **21**, 18, (1976).

B11. The Influence of Alloy Scattering on High Field Transport in Quaternary III-V Semiconductors¹. M. A. LITTLEJOHN, J. R. HAUSER, and T. H. GLISSON, N. C. State U. --This paper will present a Monte Carlo evaluation of the effects of random potential alloy scattering on high field transport properties of GaInPAs, GaInPbS, and AlInPAs. The extension of a ternary random potential model¹ to the quaternaries will be discussed. The manner in which quaternary material parameters are predicted will be presented, and the influence of the scattering potential and degree of ordering on transport properties and maximum achievable drift velocity will be addressed. A brief discussion of the effect of alloy scattering on device figures of merit will also be given.
¹J. W. Harrison and J. R. Hauser, Phys. Rev. B **13** 5347 (1976).

*Supported by the Office of Naval Research, Washington, D.C.

SESSION C: MOSTLY MOSFET's

Thursday morning, 7 July 1977; Golden Eagle Suite at 8:00 A.M.; A. Fowler, presiding

Invited Papers

C1. Transport of Hot Carriers in Semiconductor Quantized Inversion Layers.

D.K. FERRY, Office of Naval Research, Arlington, Va. (30 min.)

The transport of warm and hot carriers in quantized inversion layers has recently become of considerable interest, due in part to the quasi-two-dimensional nature of the carrier system and to the multitude of subbands present. Generally, the number of carriers in the inversion layer is sufficiently large that carrier-carrier scattering maintains a quasi-Maxwellian for the isotropic part of the distribution function, but the inter-subband interactions are sufficiently weak that each subband possesses a separate electron temperature. The treatment of carrier transport can be naturally separated into two regimes. In the first, the carriers are hot. In this regime, the transport can be found from energy and momentum balance equations and the transport differs little from a classical three-dimensional model, except in the field region in which inter-subband transfer of carriers is important. In this field range, subtle changes in the velocity-field curve are observed and significant effects are found in the microwave conductivity at frequencies on the order of the inter-subband repopulation rate. In the warm electron regime, however, for low and moderate electric fields, the degenerate nature of the carrier distribution function must be considered. Although the electron temperature concept remains valid in this regime, the agreement between theory and experiment is not good and the lack of this agreement makes it difficult to assess the physical processes occurring. The situation is complicated at low temperatures where many of the scattering mechanisms are not fully understood and the carrier densities and transport can show activation behavior. This lack of understanding is especially true in warm carrier magneto-transport. For this reason, care must be exercised in evaluating the role played by the electric field. In this paper, these various regimes are discussed and compared to the available experimental data.

C2. Review of Experimental Aspects of Hot Electron Transport in MOS Structures.
K. HESS, *Angewandte Physik and Ludwig Boltzmann Institut, Vienna, Austria.* (30 min.)

A review of carrier-mobility measurements in silicon inversion layers is given with special emphasis on high-field phenomena. Measurements reported in the literature have been performed in a range of lattice temperatures 0.03 K $\leq T \leq 300$ K for electric drain-fields $0 < E \leq 10^5$ V/cm, which heat the charge carriers up to several thousand degrees Kelvin. Numerous transport quantities have been measured in this tremendous temperature range. Special consideration is given to: conductivity, effective and Hall-mobility, magnetoresistance and Shubnikov-de Haas effect, the warm electron coefficient β and the saturation drift-velocity. Most results available are for n-channel MOS devices on (100), (110), and (111) silicon surfaces. Only few results are published for the p-channel. The results are compared with experimental findings for bulk material. The comparison shows that no drastic differences appear at temperatures above 10 K and high electric fields. Only the saturation velocity of inversion layers is lower and the temperature and field dependence of the conductivity is weaker as compared to the bulk. At temperatures below 10 K, however, activated conductivities, giant β -coefficients and in the high field region a voltage controlled negative differential resistance are observed.

Contributed Papers

C3. Far Infrared Emission From Hot Electrons in Si-Inversion Layers. E. GORNIK, *Bell Labs., Holmdel, NJ* and D. C. TSUI, *Bell Labs., Murray Hill, NJ*.--We observed narrow-band, voltage tunable, far infrared emission from hot electrons in the inversion layers of n-channel Si metal-oxide-semiconductor field-effect transistors. The hot electrons were created by applying a pulsed electric field along the channel and the radiation, emitted by the electronic transition from the two-dimensional excited E_1 subband of the inversion layer to its ground-state E_0 subband, was detected and analyzed by using a Ga-doped Ge detector in combination with several narrow-band filters. The data yielded information on the electric field dependent electron temperature and the hot electron relaxation process in the Si-inversion layers.

C4. Noise of Hot Carriers in the Channel of n Silicon Junction Gate Field Effect Transistors. D. SODINI, M. ROLLAND, G. LECOY, J.P. NOUGIER, *Universit  des Sciences et Techniques du Languedoc*.--The noise temperature $T_n(E)$ of bulk n-type silicon at 300K and 77K has been measured versus electric field. These results are used in the present paper to investigate the noise in the channel of n-type silicon J.G.F.E.T's. A simple one-dimensional modeling, previously used for determination of the I-V characteristics, is used to determine numerically the potential, and the electric field at every point of the channel. This allows to compute $T_n(E)$ and hence to deduce the noise current spectral density at the drain electrode below drain current saturation. These results are compared with the usual theoretical expression of the thermal noise, and with noise experiments performed by our group using a pulse technique in order to avoid heating of the device. The agreement between theory and experiment is satisfactory both at 300K and 77K. At 77K, the measured and computed noises are 40 to 100 times (depending on the transistors investigated) higher than those predicted by the thermal noise theory. This indicates that the excess noise is essentially due to hot carrier effects, and that other noise sources, for example generation-recombination, do not contribute significantly.

C5. Noise and Diffusion of Hot Holes in Si. C. JACOBONI, G. GAGLIANI, L. REGGIANI and O. TURCI, *Modena U.*--A recent attempt to interpret white noise data of hot holes in Si suggests the conflicting results of having an equilibrium carrier energy in the region of fields where non-ohmic behavior is clearly evident. This contradiction arises when different theoretical approaches which make use of a generalized Nyquist relation at high fields are tested on the experimental data. Since, as is shown on basic principles, white noise and diffusion describe the same physical phenomenon, a microscopic interpretation of the above experiments has been carried out by means

of the determination of the longitudinal diffusion coefficient. Agreement between theory and experiments resolves the previous contradiction and show that the Monte Carlo technique can be an effective instrument in studying noise phenomena.
I.J.L. Tandon, H.R. Bilger and M.-A. Nicolet, *Solid-St. Electron.* 18, 113 (1975).

C6. Hot Electron Studies by Tunneling. D.C.TSUI and J.M.ROWELL, *Bell Labs., Murray Hill, NJ*.--Although tunnel injection is a well-known method for creating hot electrons, tunneling techniques have only recently been employed in hot electron studies. In our earlier experiments on InAs, we measured the electron temperature directly by using superconducting tunneling, and the hot electron relaxation time by using the magneto-oscillatory effects in tunneling. In this talk, we present new results on PbTe. All these results indicate that tunneling, being sensitive to electrons close to the junction interface, is a useful tool for probing hot electron properties at the surface, and thus complementary to conventional techniques probing bulk properties.

1. J. M. Rowell and D. C. Tsui, *Phys. Rev. B* 14, 2456 (1976); D. C. Tsui, *Phys. Rev. B* 12, 5739 (1975).

C7. Current Controlled Negative Resistance in GaAs at Low Temperature. V.C. KISU, *Laboratoire de Physique des Solides, C.N.R.S., MEUDON, France*.--The ionization of shallow donor in freeze-out regime by electric field at temperature lower than some critical one lead to a current instability typical of a cooperative system. The variation of the Hall constant and the resistivity (ρ) with temperature (T) and electric field (E) have been measured on compensated n-type GaAs. - $(N_D - N_A) : 10^{14} - 10^{15} \text{ cm}^{-3}$ - the domain of instability in the (σ , T , E) diagram is similar to a first-order phase transition. The analysis of transport properties is performed in the ohmic and non-ohmic region. By assuming that mutual interaction between the conduction and the bound electrons would keep the two systems in equilibrium at the same electronic temperature T_e , the concentration of conduction electrons is calculated as a function of the applied field: the result is in better agreement with the experimental data than that obtained from the impact-ionization theory. When the energy loss for the ionization of the impurity center is taken in account, our calculation is in reasonable agreement with the experimental results, specially as regards the variation of the breakdown field with temperature and the occurrence of the instability.

C8. Measurements of the Negative Differential Resistance. + T. NEUGEBAUER, G. LANDWEHR, *Univ. W rzburg*, K. HESS, L. Boltzmann Inst. Wien, G. DORDA, *Forschungslaboratorien der Siemens AG M nchen*.+--- The voltage controlled negative differential resistivity (ndr) of n-channel MOS-transistors¹⁾ is investigated in transverse magnetic fields up to 10 T for temperatures 4.2 K $\leq T \leq 16$ K. The effect of lattice heating, which was originally made

responsible for the ndr²) has been examined by varying length and repetition rate of the current pulses. It is shown that lattice heating is not the reason for the ndr.

The ndr shows a marked dependence on the magnetic field B: the critical electric field strength at which the current drops is shifted to higher values and the peak to valley ratio is lowered with increasing B values.

Comparing these results with the characteristics of Gunn-devices in magnetic fields we suspect, that the ndr in inversion layers is also caused by hot electron effects.

1) Y. Katayama, I. Yoshida, M. Katera and K.F. Komatsubara Appl. Phys. Lett. 20, 1, 31, 1972

2) T. Sugano et al. J. of the Faculty of Eng., Univ. of Tokyo XXXII, 1, 1973

SESSION D: OPTICALLY EXCITED

Thursday afternoon, 7 July 1977; Golden Eagle Suite at 1:30 P.M.; R. Leite, presiding

Invited Papers

D 1. Picosecond Spectroscopy of Semiconductors. D.H. AUSTON,* Bell Laboratories, Murray Hill. (30 min.)

This talk will summarize recent experimental studies of carrier dynamics in semiconductors in which extremely fast temporal resolution has been achieved with the use of picosecond optical pulses. Specific topics to be discussed include transient photoconductivity, time resolved reflection and transmission of optically generated electron-hole plasmas, high density carrier transport, and Auger recombination. Time resolutions varying from 1 to 10 picoseconds have been obtained by using picosecond optical pulses both for the generation of carriers and for the measurement of their dynamics. In the case of photoconductivity, fast current transients have enabled the development of electronic devices with picosecond rise times. Present work on this topic is concerned with the influence of hot carrier thermalization rates on transient photocurrents. Optical reflectivity measurements with picosecond pulses in GaAs and CdSe show evidence of hot carrier thermalization rates of typically 0.5 eV/ps for carrier temperature in the range of 10⁴K. The influence of carrier-carrier scattering on carrier relaxation rates will also be discussed with reference to recent measurements of carrier drift mobilities by picosecond transient photoconductivity.

*This work was done in collaboration with C. V. Shank, E. P. Ippen, O. Teschke, A. M. Johnson, and S. R. McAfee.

D 2. On the Physics of Ultrafast Phenomena in Solid State Plasmas.* MARLAN O. SCULLY, University of Arizona. (30 min.)

Over the past half decade, measurements on a picosecond time scale of the nonlinear nonequilibrium optical properties of the germanium solid state plasma have been carried out in several laboratories. These measurements involve, for example, the ultrafast relaxation of optically excited nonequilibrium electron-hole distributions in semiconductors^{1,2,3} and the photoluminescence spectrum of germanium at high excitation intensities. A review of our present state of theoretical⁵ understanding of these experiments as well as the theoretical limitations and extensions will be discussed.

*Work performed in collaboration with Arthur L. Smirl and Ahmet Elci, North Texas State University and supported by the Office of Naval Research.

¹D.H. Auston and C.V. Shank, Phys. Rev. Lett. 32, 1120 (1974).

²C.J. Kennedy, J.C. Matter, A.L. Smirl, H. Weichel, F.A. Hopf, and S.V. Pappu, Phys. Rev. Lett. 32, 419 (1974).

³A.L. Smirl, J.C. Matter, A. Elci, and M.O. Scully, Opt. Comm. 16, 118 (1976).

⁴H.M. van Driel, A. Elci, J.S. Bessey, and M.O. Scully, Solid State Comm. 20, 837 (1976).

⁵A. Elci, M.O. Scully, A.L. Smirl, and J.C. Matter, Phys. Rev. B (to be published).

Contributed Papers

D3. The Role of Phonons and Plasmons in Describing the Pulsewidth Dependence of the Transmission of Ultra-short Optical Pulses Through Germanium. *ARTHUR L. SMIRL, W.P. LATHAM, AHMET ELCI, North Texas State University, and JOHN S. BESSEY, University of Arizona.--Recently, we developed a first principles model¹ that accounts for the generation and transient behavior of dense electron-hole plasmas produced in germanium by picosecond optical pulses. In this model the temporal evolution of the hot electron plasma is sensitive to the relative strengths of the electron-phonon relaxation and the plasmon emission. The agreement between this model and early experiments is substantial. However, further experiments, involving optical pulses of varying width, have indicated that the initial model is incomplete. In this talk we emphasize the dependence of the optical properties of the Ge plasma on the electron-phonon coupling constant and the energy band structure, and we suggest modifications to the original model that produce agreement with the more recent experiments.

¹A. Elci, M.O. Scully, A.L. Smirl, and J.C. Matter, Phys. Rev. B (to be published).

*Supported by Office of Naval Research.

D4. Optical Studies of Hot Electrons in Vapor Phase Epitaxially Grown Ge Films. JOHN S. BESSEY, BRUNO BOGACCHI, K. AL-KHATEEB, and M.O. SCULLY, University of

Arizona, and F.C. JAIN, University of Connecticut -- Over the last few years several studies have been made on the non-linear interaction of ultrashort optical pulses with semiconductors. These have been primarily carried out on single crystal thin films of germanium ground and polished from bulk intrinsic material. These samples have been limited to thicknesses of the order of 5 μ m due to mechanical problems inherent in the sample preparation. We now present the results of measurements extending the previously developed techniques to Ge samples of thicknesses from around 8 to less than 1 μ m obtained by vapor phase epitaxial deposition on GaAs substrates. These show marked variations in properties which will be discussed within the framework of the model proposed by Elci et al.¹

¹A. Elci, M. O. Scully, A.L. Smirl, J.C. Matter, Phys. Rev. B (to be published).

*Permanent address: Al Hazen Institute, Baghdad, Iraq.

D5. Absorption Spectrum of Optically Pumped GaAs: Band Filling and Hot Electron Effects. R. F. LEHENY and JAGDEEP SHAH, Bell Labs, Holmdel, N. J.--Measurements of transmission spectra through thin layers of GaAs ($\approx 0.5 \mu$) in the presence of an intense optical pumping by a tunable infrared (8100-7500Å) laser are described. Effects of band filling and carrier heating due to the optical pumping can be determined directly from changes in the transmission spectra. Carrier temperatures of $\approx 40^\circ$ K for samples immersed in liquid helium are deduced from fitting absorption spectra for a pump wavelength of ≈ 8000 Å.

D6. Properties of Hot Photoexcited Holes in Cu-doped Germanium at Low Temperature. A. NOGUERA, *Universidad de los Andes, Venezuela* and C. J. HEARN, *Warwick U.* -- A theoretical study is made of the properties of hot photoexcited holes in Cu-doped Germanium as a function of the lattice temperature and compensation density (N_A). Numerical solutions of the rate equation, obtained by an iterative technique, give the steady-state energy distribution of hot photoexcited holes due to approximately blackbody room temperature radiation. Considering only a spherical heavy-hole band, simple acoustic deformation scattering and instantaneous optical phonon emission it is found that for the lowest values of N_A the energy

distribution function is approximately Maxwellian and gives a good fit with experimental photoHall mobilities.¹ For higher values of N_A , a spherical light hole band is included in our calculations and this involves the use of a two-parameter deformation potential for inter- and intra-valley transverse and longitudinal scattering, and also instantaneous inter- and intra-valley optical scattering. The experimental photo-Hall mobilities then can be used to give information on the deformation potential parameters for the valence band of Ge which cannot be derived from equilibrium transport measurements.

¹P. Norton and H. Levistein, *Phys. Rev.* **6**, 478 (1972).

Invited Papers

D 7. Field Effects for Laser Excited Carriers. C.J. HEARN, *Warwick University, Coventry.* (20 min.)

D 8. Radiative Spectra from Hot Photocarriers. R.C.C. LEITE, *UNICAMP, Campinas, Brazil.* (20 min.)

Radiative recombination from non-equilibrium carriers in semiconductors are compared with single particle scattering in GaAs. The Raman scattering data is obtained by two photon absorption in bulk material whereas the photoluminescence spectra are obtained by regular one photon absorption. The results are in close agreement with current theories.

D 9. Photocarrier Thermalisation by Laser Excitation Spectroscopy. C.C. WEISBUCH, *Ecole Polytechnique, Palaiseau, France.* (20 min.)

Lineshapes of luminescence lines in photoexcited semiconductors provide a convenient way to measure effective temperatures of hot electrons and excitons. Excitation spectroscopy of such lines, i.e. the study of the variation of intensity and lineshape of these lines with varying exciting photon energy permits to follow in a very detailed manner the energy relaxation path of hot photocreated electrons. This has been performed in GaAs using a c.w. tunable dye laser and leads to the observation of an oscillation of electronic temperature with changing exciting photon energy. This is due to the efficient energy relaxation by L.O. phonon emission for those electrons created in the conduction band with a initial kinetic energy equal to an integer number of L.O. phonons. The simultaneous oscillations of electronic and excitonic densities, temperatures and lifetimes show the dependence of many quantities such as exciton formation time, exciton thermalisation etc... on the effective electronic temperature. It also provides new experimental insight on oscillatory photoconductivity phenomena, as it separately gives information on carrier density and temperature.

Contributed Papers

D10. Mean energy of photoexcited hot electrons in high magnetic fields.

C. LEWINER and D. CALECKI, *Groupe de Physique des Solides de l'E.N.S., Université Paris VII, Tour 23, 2 place Jussieu, 75005 Paris (France).*

Several authors^{1,2} have determined the mean energy of a photoexcited electron gas in the absence of magnetic field. Assuming a Maxwellian distribution for the main electrons, they used the power balance equation to find the electron temperature T_e .

Noting that, when a strong magnetic field is applied, the electron-electron collision integral vanishes in the extreme quantum limit³, we derive a theoretical expression for T_e using a similar approach. Radiative recombination and various scattering processes (by optical and acoustical phonons) are considered and the dependence of T_e on magnetic field, lattice temperature and laser frequency excitation is studied.

¹R. Ulbrich, *Phys. Rev. B* **8**, 5719 (1973).

²V.L. Komolov, I.N. Yassievich, *Sov. Phys. Semicond.* **8**, 732 (1974).

³A.M. Zlobin, P.S. Zyryanov, *Sov. Phys. J.E.T.P.* **31**, 513 (1970).

D11. Energy Relaxation of Photoexcited Hot Electrons at Very Low Temperatures. Y.B. LEVINSON, *Landau Inst. Theor. Phys., Moscow.* -- At very low temperatures $T \ll T_e$ and electron energies $\epsilon \sim 1/2 m^* v_s^2$ (m^* - effective mass, v_s - sound velocity) neither of the known energy relaxation mechanisms is operative. In this energy region not only optical phonon emission is forbidden, but acoustical phonon emission is also. Such a situation appears in

experiments at liquid helium temperatures when electrons in quantizing magnetic fields are excited by laser light. For example, in Ge with $H \parallel (111)$ the longitudinal mass $m = 1.64$ and $m^* = 2.8K$. We have shown that in the passive region $\epsilon < 1/2 m^* v_s^2$ the energy relaxation is due to a two-

step scattering: the electron in some state in the passive region first absorbs an acoustical phonon and passes to the active region $\epsilon > 1/2 m^* v_s^2$; then the electron emits a phonon and returns to a new state in the passive region. Such a two-step scattering is not a two-phonon process since the intermediate state is a real one, and not a virtual one. To some extent, it is similar to the two-step optical phonon scattering. The two-step acoustical phonon energy relaxation rate is of the order of $\tau^{-1} = \omega_m^2 \exp[-a(m^* v_s^2/T)]$ where "a" is the number of the order of unity, and $\omega = 10^{-3} - 10^{-4}$ is the nondimensional electron-acoustical phonon coupling constant.

D12. Hot Photo-carrier and Hot Electron Effects in PN Junction M. UMENO, Y. SUGITO, T. JIMBO, H. MATTORI, and Y. AMEMIYA, *Nagoya U. Nagoya, Japan* -- When a pn junction of semiconductor (with bandgap energy E_g) is illuminated by light beam (with photon energy $h\nu$) in the condition of $E_g > h\nu$, such as in Ge pn junction illuminated by CO₂ laser beam, an electromotive force (emf) was induced between the terminals of the pn junction, which indicated the opposite polarity to the ordinary photovoltaic effect like in a solar cell. Such an anomalous photovoltaic phenomenon was discussed with many other photovoltaic mechanisms, and it was explained by an optically excited hot carrier effect, through the following experiment with electrical excitation. Using a rod of n- or p-type Ge with a pn junction at the surface of its center and an ohmic contact at each terminal of the rod, the same kind of phenomena was observed when electric field is applied along the length of the rod. The vertically induced voltage or current had the same polarity in spite of the reverse change of the applied field, and increases with increasing the applied field strength. The vertically induced emf was caused by warm or hot carriers crossing the potential barrier of the pn junction, which is very sensitive to the departure from thermally equilibrium velocity distribution of carriers.

SESSION E: QUANTUM TRANSPORT

Friday morning, 8 July 1977; Golden Eagle Suite at 9:00 A.M.; C. Jacoboni, presiding

Invited Paper

E1. Hot Electron Quantum Magneto-Transport. J.R. BARKER, Warwick University, United Kingdom. (30 min.)

A review is given of recent experimental findings and theories on hot electrons in quantising magnetic fields. Particular attention is paid to instability phenomena and the magnetophonon effect.

Contributed Papers

E2. Quantum Theory of Nonohmic Galvanomagnetic Effects in Semiconductors. H.W. SPECTOR, I.I.T. and V.K. ARORA, Univ. of Riyadh. -- We have extended the quantum transport formalism developed by Arora and Peterson¹ to calculate the magnetoresistance of semiconductors by taking into account nonohmic effects. Our calculations yield expressions for the magnetoresistance which are valid for arbitrary electric field and which reduce to the correct ohmic results for low electric fields. Although our expressions are valid for arbitrary electric fields, they have to be supplemented by an energy balance equation to take electron heating into account and by kinetic equations which yield the nonequilibrium phonon distribution when acoustic phonon scattering is dominant and we have acoustoelectric amplification. An expression for the nonohmic magnetoresistance is obtained in the quantum limit when acoustic phonon scattering is dominant.

¹V.K. Arora and R.L. Peterson, Phys. Rev. B12, 2285 (1975).

E3. Application of a new high field quantum magneto-transport theory for polar semiconductors. F. BELEZNAY, M. SERENYI, Res. Inst. Techn. Phys., Budapest, Hungary. -- High field quantum magneto-transport theory based on Feynman's Path Integral method¹ has been derived. The first approximation gives implicit relations between applied field and drift velocity of electrons in magnetic field. Calculations for InSb at 77K explains measured low field longitudinal magnetoresistance², low and high field transversal mobility data³ and warm electron coefficient⁴ for different magnetic fields and predicts high field longitudinal properties. The validity of our approximation in frame of the general transport quantum theory⁵ is discussed. Extension of our calculations for intermediate and strong coupling cases, initiated by recent measurements on Silver Halides, are in progress.

¹K.K. Thornberg and R.P. Feynman, Phys. Rev. B1, 4098.

²M. Tokumoto, C. Yamanouchi, and K. Yoshihiro, J. Jap. Phys. Soc. 37, 878 (1974).

³H. Fujisada, S. Kataoka, and A.C. Beer, Phys. Rev. B3, 3249 (1971).

⁴T. Shirakawa, C. Hamaguchi, and J. Nakai, J. Jap. Phys. Soc., 35, 1098 (1973).

⁵J.R. Barker, J. Phys. C, 6, 3663 (1973).

E4. Impurity Spectroscopy on Tellurium by Means of Magnetoresistance Measurements under Nonohmic Conditions. K. von KLITZING, U. WURZBURG. -- Low temperature magnetoresistance measurements on weakly doped tellurium samples ($p \sim 10^{15} \text{ cm}^{-3}$) show a large number of structures which appear only under nonohmic conditions. Depending on the electric field strength and the chemical nature of the impurities, different types of structures in the magnetoresistance are visible. The most remarkable effect is the appearance of sharp maxima in the magnetoresistance (half-width $\Delta B \sim 0.07 \text{ T}$) which show up at relatively low electric fields of about 1 V/cm. The magnetic field positions of these peaks are correlated with the chemical nature of the impurities. The resonance appears for the different impurities at $B = 3.41 \text{ T}$ (Bi), $B = 3.61 \text{ T}$ (Sb), and $B = 3.77 \text{ T}$ (As) (Bic). Further structures in the magnetoresistance under hot carrier conditions are correlated with a resonance between the lowest impurity excitation energy and the cyclotron resonance energy. From hot magnetophonon measurements, impurities with quite different binding energies could be identified.

E5. Electric-Field Dependence of the Positions and Amplitudes of Magnetophonon Oscillations in n-InSb at 77 K. H. KAHLERT, D. G. SEILER, North Texas State U., and J. R. BARKER, U. of Warwick, Coventry, U. K. -- The influence of pulsed electric fields on the magnetophonon structure in the transverse and longitudinal magnetoresistance of n-InSb at 77 K has been reexamined using a magnetic field modulation technique. For the transverse configuration, a shift to higher magnetic fields with increasing electric field is observed for extremal positions up to $N = 8$. The amplitudes decrease monotonously and disappear at about 60 V/cm for $N=3$. In the longitudinal case the extrema shift to lower magnetic fields as the electric fields is increased. In contrast to the transverse case, the amplitudes increase by a factor of 2 up to 15 V/cm, and then either decrease or become saturated, depending on the harmonic number of the extremum under consideration. These experimental results are compared to calculations based on a quantum kinetic equation approach and to predictions obtained from a simplified analytical theory.

*Work supported in part by the Office of Naval Research

**On leave from Ludwig Boltzmann Institut fuer Fest-korperphysik and Institut fuer Angewandte Physik, Universitaet Wien, Austria

E6. Hot Electron Energy Recombination in Quantizing Magnetic Fields. W. MÜLLER, F. KOHL, H. PARTL, and E. GÖRNIK^{*}, Technische Universität Wien, A-1040 Vienna, Austria. -- We have studied the radiative recombination of hot electrons between Landau levels¹ in n-InSb at 4.2 K in order to obtain detailed information on the hot carrier distribution function and energy recombination processes. The measurements were performed in the magnetic field range from .5 to 3.0 T on various samples with different free electron and total impurity concentration. The hot electron occupation numbers of the first Landau level were derived in dependence of the electric and magnetic field applied. Information on the electronic lifetime in the first Landau level was obtained from the direct observation of the electric field response of the recombination radiation intensity. Electron lifetimes of less than 10 ns, which are found experimentally, can be explained by an Auger-like recombination process. The hot electron distribution function has a nearly Maxwellian shape in good agreement with an improved theoretical approach taking electron-electron interaction into account.

^{*}Present address: Bell Telephone Laboratories, Holmdel, N.J.

¹E. GÖRNIK, Phys. Rev. Lett. 29, 595 (1972).

E7. Optical Field Induced Intervalley Transfer and Gunn Oscillations in GaAs. A. V. NURMIKKO and B. D. SCHWARTZ, Brown U. -- Intense infrared laser fields near 10 μm wavelength have been used to enhance intervalley transfer of conduction band electrons and to trigger Gunn instabilities in n-type GaAs on nanosecond timescale. In these experiments samples in the form of thin epitaxial layers ($n = 8 \times 10^{14} \text{ cm}^{-3}$, $\mu(300^\circ\text{K}) = 6700 \text{ cm}^2/\text{V sec}$) have been subjected to simultaneous excitation by a dc-field and a laser field from a mode-locked high pressure CO₂ laser. For optical fields in the range of a few kV/cm and exceeding a critical threshold value, Gunn oscillations can be initiated and controlled by the subnanosecond laser pulses. In addition, the experimental technique has been used to study the formation and the dynamics of the instabilities with high temporal resolution. An attractive device application is the

use of infrared radiation for high-speed optical control of Gunn microwave sources.

* Supported by the Materials Research Laboratory at Brown University.

E8. CO₂ Laser-Induced Hot Electron Effects in n-InSb. B.T. MOORE, D.G. SEILER, and H. KAHLERT, North Texas State U. -- The influence of a 2- μ sec wide CO₂ laser pulse on the Shubnikov-de Haas (SDH) effect in a $1.4 \times 10^{15} \text{ cm}^{-3}$ sample of n-InSb has been investigated at a lattice temperature of 1.8K. During the time the sample is illuminated the SDH amplitudes are found to decrease with increasing laser power. For a peak incident power of about 1 watt, the SDH oscillatory behavior corresponds to that measured at 3K for the non-illuminated sample. For peak powers greater than 2 watts, the SDH amplitudes are damped out, corresponding to a non-illuminated temperature greater than 4.2K. These results form the first direct and quantitative evidence for electron heating induced by CO₂ laser radiation and permit the evaluation of a phenomenological energy relaxation time.

*Work supported in part by the Office of Naval Research.

* On leave from Ludwig Boltzmann Institut fuer Fest-

koerperphysik and Institut fuer Angewandte Physik, Universitaet Wien, Austria

E9. Growth of an Electron-Hole Liquid in CdSe?

T. DALY, and H. MAHR, Cornell U. -- Luminescence spectra of highly photo excited CdSe platelets were taken at 1.8°K at various delay-times after pulse excitation by 10 ps duration light pulses from a c.w. mode locked dye laser. During the first 150 ps after excitation a considerable narrowing and a small shift of the maximum position of a main luminescence feature centered at about 6820Å takes place. A narrow band of 6 meV bandwidth (FWHM) persists up to 2 nsec after excitation with unchanged width or shape although its intensity decays with a time constant of about 500 ps. We tentatively interpret these results as being due to the growth of an electron-hole liquid phase from an initial, denser and hotter plasma. A quantitative fit of the results to a theoretical line shape function of recombination radiation in CdSe is being carried out.

* This work is supported by a National Science Foundation Grant to Cornell's Material Science Center and by the U. S. Office of Naval Research.

SESSION F: MAINLY BULK TRANSPORT

Friday afternoon, 8 July 1977; Golden Eagle Suite at 1:30 P.M.; H. Heinrich, presiding

Invited Papers

F 1. High Field and Breakdown Effects in SiO₂. R.C. HUGHES, Sandia Laboratories, Albuquerque. (30 min.)

Amorphous SiO₂ is widely employed as an insulator in applications where very high electric field standoff is required; an example is the metal-oxide-semiconductor transistor. The ultimate breakdown strength of the bulk material depends on the high field behavior of excess electrons and holes. One mechanism for dielectric failure in the bulk is the avalanching of the excess carriers when the electric field is too high for energy loss mechanisms to stabilize the carrier drift velocity. We have measured the high field transport of both electrons and holes in SiO₂ in fields up to $5 \times 10^6 \text{ V/cm}$, and find intrinsic mechanisms for energy loss to the lattice by both electrons and holes which account for the stability of the drift velocity at these very high fields. In amorphous SiO₂ electrons are quite free in spite of the disorder and have a mobility of about $20 \text{ cm}^2/\text{V-sec}$ at room temperature which is in good agreement with theory for scattering of the electron by longitudinal optical (LO) phonons. We have measured the drift velocity of the electrons as a function of field and find that above $5 \times 10^5 \text{ V/cm}$ the drift velocity begins to saturate, which is in agreement with a theory for electron energy loss in polar materials by emission of LO phonons. Measurements of electron yield from pulsed ionizing radiation indicate that no avalanche multiplication of electrons is occurring up to at least $6 \times 10^6 \text{ V/cm}$; the theory of Thornber and Feynman predicts stability up to about 10^7 cm/sec . Experimental results from other laboratories for dark currents, electronic switching phenomena and laser induced breakdown, which are in rough agreement with the ideas of the dominance of LO phonons in the high field behavior of electrons, will be discussed. We have strong experimental evidence that holes in SiO₂ form small polarons within a few vibrational periods ($< 10^{12} \text{ sec}$). The mobility of the small polarons has been measured with nanosecond time resolution and found to be very low and thermally activated. Fields up to $5 \times 10^6 \text{ V/cm}$ do not change the mobility; the self-trapping of the hole is clearly a strong energy loss mechanism which prevents avalanching of the holes even at these high fields.

*Work supported by U.S. Energy Research and Development Administration.

F 2. High Field Electronic Conduction in Insulators. K.K. THORNBUR, Bell Laboratories, Murray Hill. (30 min.)

The quantum theory of electronic transport phenomena in large electric fields in highly dissipative media is critically examined. Serious conceptual problems and computational difficulties arise because neither the field nor the dissipation can be treated as a perturbation. We review a decade-old calculation of the velocity acquired by an electron in a finite electric field in a polar crystal and subsequent work which expanded our understanding of our method and results. A key feature of the earlier work was that in a single curve of electric field versus velocity, all the expected phenomena appeared, including a threshold field for producing hot electrons, in quantitative agreement with experiment, and a decreasing rate of energy loss with velocity for very fast electrons. A more recently studied problem, that of electron acceleration below the threshold field will be discussed. This problem is very important since such acceleration is the necessary precursor of ionization and breakdown. The physical significance of dissipation processes far from thermal equilibrium will also be mentioned.

Contributed Papers

F3. High Field Collision Rates in Polar Semiconductors. J.R. BARKER, Warwick U., U.K. -- Quantum trans-

port calculations for hot electrons in polar semiconductors reveal a strong distortion of the high-momentum transfer process by interference of the electric field with the collisions. The effect is analysed in terms

of the non-Markovian nature of the conduction process and is dependent upon a finite collision duration. Implications for high field polaron transport in insulators are discussed.

F4. Hot Electrons, Impact Ionization and Dielectric Breakdown in Thin Film SiO_2 . P.M. SOLOMON, IBM, Thomas J. Watson Research Center.--Vacuum electron emission measurements have been carried out on Si- SiO_2 -Au tunnel structures to study the hot electron energy distribution

in the oxide. Electrons of energies up to 8eV relative to the gold counter electrode vacuum level have been observed at oxide fields up to 8 MV/cm. Electron temperatures, based on a quasi Maxwellian distribution were in excess of 1.5eV and increase with applied field, supporting the possibility of bandgap impact ionization in the oxide. Impact ionization is required by some recent theories for breakdown in SiO_2 and offers an explanation for experimentally observed current instabilities and positive charging of the oxide at high fields.

Invited Paper

F5. Hot-Electron Emission from Silicon Dioxide.
T.H. NING, IBM Thomas J. Watson Research Center, Yorktown Heights. (30 min.)

Recent progress in the study of hot-electron emission from silicon into silicon dioxide is discussed. Experimental techniques include avalanche injection using gated diodes and MOS capacitors, nonavalanche injection using IGFET structures with an underlying supply p-n junction, and optically induced injection using silicon-gate IGFET structures. IGFET structures allow the fields in the SiO_2 layer and in the silicon depletion region to be varied independently. In addition, IGFET structures of reentrant geometry allow absolute emission probabilities of the hot electrons to be determined. Such absolute emission characteristics are useful not only for designing silicon devices but also for quantitative testing of theoretical models of the emission process. Several mechanisms of importance in the emission process have been identified, including Schottky lowering of the emission barrier, scattering of hot electrons in the image-force potential well in the SiO_2 layer, tunneling of hot electrons, and the effect of lattice temperature on electron heating. There is also experimental evidence of the dependence of the hot-electron energy distribution on electric field gradient. At present, only phenomenological models based on the lucky-electron concept have been developed to the point where quantitative comparison with experimental results is possible. The essential features of these models are discussed.

Contributed Papers

F6. Semiconductor Surface Emission of Hot Electrons*.
R. R. TROUTMAN, IBM, Essex Junction, VT. A new emission model, based on a probabilistic treatment of electron trajectories, has been developed for hot electron emission from a semiconductor surface. Primary electrons, generated thermally or optically, are heated by a normal electric field and cooled by phonon collisions and by impact ionization. Unlike the case in previous models, the semiconductor field need not be uniform, and multistage phonon processes are included. The model provides hot electron energy distributions in the semiconductor and as they are emitted. It shows that the most probable trajectory of an emitted electron is not one of zero collisions (as assumed in the analysis of Vervey et al.¹), but one involving the generation of many optical phonons. The model, used together with photo-excited hot electron measurements (as developed by Ning and Yu²), also provides an accurate method for determining phonon and ionization mean free paths.

*Submitted by E.E. Gardner

¹J.F. Vervey, et al., JAP 46, 2612 (1975).

²T.H. Ning and H.N. Yu, JAP 45, 5373 (1974).

F7. Interrelationship between Impact Ionization, Velocity Saturation and Cascade Process in Semiconductor via a Markov Matrix Modelling*, R. Chwang, and C.R. Crowell, U of Southern California--Hot carrier impact ionization (described in terms of the mean free path λ_p for optical phonon scattering, $\langle E_p \rangle$, the average energy loss per phonon collision and E_{th} , the ionization threshold obtained from band structure¹); the velocity-field relationship (characterized mainly by λ_p and $\langle E_p \rangle$); and the mean and variance (i.e. Fano factor) of the energy per electron-hole pair production in the cascade process (which calibrates the energy dependence of the ionization mean free path $\lambda_i(E)$ in terms of λ_p) are correlated as a function of temperature. This study uses a finite Markov chain formulation based on transition matrices defined by the optical phonon and ionization scattering probabilities in energy space. For isotropic scattering in nonpolar semiconductors, this approach facilitates parametric (λ_p and $\lambda_i(E)$) studies of both transient and steady state transport properties of the hot carriers. Results are

in excellent agreement with available experimental data for Si and Ge.

¹C.L. Anderson and C.R. Crowell, Phys. Rev. B5, 2267 (1972).

*Research supported by U.S. Army Research Office under Grant No. DAAG 29-75-0002.

F8. Electron Transport and Ionization in Silicon at High Fields. H.P.D. LANYON, Worcester Polytechnic Institute.--The saturated drift velocity measured for electrons at high fields is inconsistent with Shockley's model for impact ionization in silicon. It is explained in terms of a field-dependent mean free path for high energy phonon creation in the electric field direction, electrons creating a high energy phonon as soon as they have acquired sufficient energy from the field. Assuming that the electron wavepacket travels at the saturated drift velocity without dispersion, it can be shown that the increased scattering rate at high fields must result in a large spread in the carrier energy. If a drifted Maxwellian distribution is assumed, a unique expression can be obtained for the carrier temperature T^* which is in good agreement with the measured field dependence of the ionization coefficient. In this model, a cylindrical hot carrier distribution must be assumed with the hot carrier energy in a plane perpendicular to the applied field. Exact calculations of the magnetoresistance of such a distribution can be made verifying that the drift velocity is indeed saturated.

F9. Electric Field Orientation and Magnitude Dependence of Electronic Transitions Induced by Hot Carrier Impact Ionization in Semiconductors: GaAs. T.P. PEARSALE, LCR Thomson/CSF, F. CAPASSO*, R.E. NAHORY, Bell Laboratories, Murray Hill.--We have measured the impact ionization rates for both electrons, (a), and holes (b), as a function of electric field at 300°K for three principal orientations of electric field in GaAs: $\langle 100 \rangle$, $\langle 110 \rangle$, and $\langle 111 \rangle$. We show for the first time that the ionization rates, and more specifically their ratio $K=a/b$, can display a pronounced dependence upon both the orientation and magnitude of the electric field. Our measurements were made for $3 \times 10^5 \text{ V.cm}^{-1} < E < 6 \times 10^5 \text{ V.cm}^{-1}$. In this range $K \approx 1$ for E in the $\langle 111 \rangle$, $K \approx 1$ for E in the $\langle 110 \rangle$, and in the $\langle 100 \rangle$, $K \approx 1$ for $E < 4 \times 10^5 \text{ V.cm}^{-1}$ and $K \approx 5$ for $E > 5 \times 10^5 \text{ V.cm}^{-1}$. These results can be understood by considering in detail the electronic band structure of GaAs, and how

it determines the transitions associated with impact ionization by hot carriers. Measurements of the temperature and bandgap dependence of impact ionization in GaAs will be used to further clarify this relationship.

*Permanent address: Fondazione <<UGO Bordonio>>, Rome, Italy.

F10. Negative Electron Diffusivity in High Electric Fields. D. CHATTOPADHYAY and B.R. NAG, Inst. of Radio-physics and Electronics, India.--Relation between current fluctuations and diffusion constant for near-equilibrium conditions suggests that the diffusion constant cannot be negative. In the presence of strong electron-electron collisions in the non-equilibrium state as in hot-electron conditions, it is, however, found that this general result may not be valid and the diffusion constant may be negative. Nag had given a formula for parallel diffusion constant from phenomenological considerations, which explains the experimental results of silicon. It also follows from this formula that under certain conditions the diffusion constant may be negative, even if the differential conductivity is positive. This paper presents results of a detailed study of the problem starting from the Boltzmann equation and using a moment method. It is found that the diffusion constant is positive for predominant acoustic phonon, polar optical phonon or impurity atom scattering.

But the constant may be negative when effects of non-parabolicity are important and energy relaxation is limited by non-polar optical phonon scattering but the momentum relaxation is dominated by impurity atom scattering.

F11. Impact Ionization of Shallow Donors in Germanium, 4°K-13.5°K. W. PICKIN, ENEP-Cuautitlán, UNAM.--Rate coefficients for phonon and impact processes, for given electric field E , are calculated in the effective-mass approximation for transitions among donor energy levels and between these levels and the conduction band, using Stratton, equipartition, and Maxwellian distribution functions in the band; downward transitions are treated explicitly, without use of detailed balance. The rate equations for the system of band and donor levels are solved to give an equation for electron concentration $n(E)$ in the band; this is interpreted in terms of the concept of "sticking probability", which is thus clarified and extended. The effect of the donor excited states is shown to be significant; regimes in which it is dominant, and in which it can lead to S-breakdown, are identified. Error estimates are given, based on explicit variation of uncertain donor parameters. *Address for correspondence: Milán 38-A403, Col. Juárez, México, 6, D.F., México.

SESSION G: RUMP SESSION ON FUTURE TRENDS

Saturday morning, 9 July 1977; Forum Room 411 at 9:00 A.M.; H. Kroemer, presiding

AUTHOR INDEX

Abe, K. -B4
Adams, A.R. -B5
Al-Khateeb, K. -D4
Amemiya, Y. -D12
Antypas, G.A. -B6
Arora, V.K. -E2
Auston, D.H. -D1
Barker, J.R. -E1, E5, F3
Bauer, G. -A3
Beleznyay, F. -E3
Bessey, John S. -D3, D4
Boltzmann, L. -C8
Bosacchi, Bruno -D4
Buettiker, M. -B8
Burke, J.R. -B6
Calecki, D. -D10
Capasso, F. -F9
Chattopadhyay, D. -F10
Chwang, R. -F7
Crowell, C.R. -F7
Czubatyj, W. -B3
Daly, T. -E9
Dorda, G. -C8
Elol, Ahmet -D3
El-Sabbahy, A. -B5
Ferry, D.K. -B6, C1
Gaglianti, G. -C5
Glisson, T.H. -B7, B11

Gornik, E. -C3, E6
Grubin, H.L. -B2
Hattori, H. -D12
Hauser, J.R. -B7, B11
Hearn, C.J. -D6, D7
Heinrich, H. -B9
Hess, K. -C2, C8
Hilsum, C. -A1
Houston, B.B. -B6
Howlett, W. -A5
Hughes, R.C. -F1
Inoue, M. -A4
Inuishi, Y. -A4
Jacoboni, C. -C5
Jain, F.C. -D4
Jantsch, W. -B9
Jimbo, T. -D12
Kahlert, H. -E5, E8
Kieu, V.C. -C7
Kimura, T. -B4
Kobayashi, T. -B4
Kohl, F. -E6
Kroemer, H. -B1
Landwehr, G. -C8
Lanyon, H.P.D. -F8
Latham, W.P. -D3
Lecoy, G. -C4
Leheny, R.F. -D5

Leite, R.C.C. -D8
Levinson, Y.B. -D11
Lewiner, C. -D10
Littlejohn, M.A. -B7, B11
Mahr, H. -E9
McHugh, T.M. -B2
Moore, B.T. -E8
Müller, W. -E6
Nag, B.R. -F10
Nahory, R.E. -F9
Neugebauer, T. -C8
Ning, T.H. -F5
Noguera, A. -D6
Nougier, J.P. -C4
Nurmikko, A.V. -E7
Parti, H. -E6
Pearsall, T.P. -F9
Pickin, W. -F11
Reggiani, L. -C5
Restorff, J.E. -B6
Rolland, M. -C4
Rowell, J.M. -C6
Rosenbergs, J. -B9
Schwartz, B.D. -E7
Scully, Marian O. -D2
Scully, M.O. -D4
Seiler, D.G. -E8, E8
Serenyi, M. -E3

Shah, Jagdeep -A6, D5
Shaw, M.P. -B3
Shenderovskij, V.A. -B10
Shirafuji, J. -A4
Shur, M.S. -B3
Smirl, Arthur L. -D3
Sodini, D. -C4
Solomon, P.M. -F4
Spector, H.N. -E2
Sugito, Y. -D12
Takahara, K. -B4
Takenaka, N. -A4
Thomas, H. -B8
Thornber, K.K. -F2
Tomchuk, P.M. -B10
Troutman, R.R. -F6
Tsui, D.C. -C3, C6
Turci, O. -C5
Ulbrich, R.G. -A7
Umeno, M. -D12
von Klitzing, K. -E4
Wassef, Wafik A. -A8
Watson, Thomas J. -A2
Weisbuch, C.C. -D9
Yamamoto, K. -B4
Young, M.L. -B5
Zukotysanski, S. -A5

INTERNATIONAL CONFERENCE ON HOT ELECTRONS - July 6-9, 1977

- ABE, Kenji - Dept. of Electronics, Kobe University, Kokko, Nada, Kobe 657, Japan
 ABRAMSON, D. A. - Physics, Purdue U., W. Lafayette, Ind. 47907
 ADAMS, A.R. - Physics, Univ. of Surrey, Guildford, Surrey GU2 5XH, UK
 AUKERMAN, L.W. - 949 Rowell, Manhattan Beach, CA 90266
 AUSTON, D. - Bell Labs, 600 Mountain Ave., Murray Hill, NJ 07974
 BARKER, J.R. - Physics, U. of Warwick, Coventry Warwickshire CV4 7AL, UK
 BATE, R.T. - Texas Instruments, 3106 Kristen Ct., Garland, TX 75042
 BAUER, G. - Experimentelle Physik IV, U. Ulm, Oberer Eselsberg, D-79 ULM, FRG
 BESSEY, J.S. - U. of Arizona, Optical Sciences Center, Tucson, Arizona 85721
 BLASKE, Allen - VARO Semiconductors, Inc., New Products Div., 1000 N. Shiloh, Garland, TX 75040
 BLEDSOE, H. - 1304 Keeling, Odessa, Texas 79763
 BRANDENBURG, R. - 10820 Leota Drive, Dallas, TX.
 BLUDAU, W. - Dept. K32/28I - IBM, 5600 Cottle Road, San Jose, Ca. 95193
 BUETTIGER, M. - Inst. fur Physik der Universität Basel, Theoretische Physik, Klingelbergstrasse 82, Switzerland
 CALECKI, D. - GPS Tour 23, Université Paris VII, 2 Place Jussieu 75005, Paris
 CONWELL, E. - Xerox, Xerox Square W114, Rochester, N.Y. 14644
 COMPAAN, A.D. - Physics, Kansas State U., Manhattan, Kansas 66506
 COLEMAN, J. - Texas Instruments, P.O. Box 5936, Dallas, Texas 75222
 COLLINS, C. - University of Texas, P.O. Box 688, Richardson, Texas 75080
 COOPER, L.R. - ONR, Arlington, Virginia 22217
 CROWELL, C.R. - U. of Southern Ca., Dept. of Materials Science, Los Angeles, CA 90007
 DAHIYA, Jai - Physics, North Texas State University, Denton, Texas 76203
 DAS, P. - Rensselaer Polytechnic Inst., Troy, New York 12181
 DEERING, W.D. - Physics, North Texas State University, Denton, Texas 76203
 DINGLE, R. - Bell Laboratories, 600 Mountain Ave., Murray Hill, New Jersey 07974
 DOCKERTY, R. - IBM Building, 300-425, Dept. 957, Hopewell Jct, New York 12533
 DOWDY, D. - Physics, North Texas State University, Denton, Texas 76203
 DUGUAY, M.A. - Bell Laboratories, Holmdel, New Jersey 07733
 ELCI, Ah. - Physics, North Texas State University, Denton, TX 76203
 EL-SABBAHY, A. - Physics, Surrey U., Guildford, Surrey, England GU2 5XH
 ENGELAGE, J.M. - Physics & Astronomy, LSU, Baton Rouge, LA 70803
 FERRY, D. - ONR, Arlington, Virginia 22217
 FOSTER, B.P. - Physics, North Texas State University, Denton, Texas 76203
 FOWLER, A. - IBM Watson Research Center, Yorktown Heights, New York 10598
 GILLESPIE, S. - IBM, Essex Junction, Vermont 05452
 GLISSON, T.H. - North Carolina State University, Raleigh, North Carolina 27607
 GOEBEL, E.O. - U. of Stuttgart, Pfaffenwaldring 57, D-7000, Stuttgart 80, Germany
 GOODWIN, M. - Physics, North Texas State University, Denton, TX 76203
 GRUBIN, H.L. - United Technologies Research Center, East Hartford, CT 06108
 GRUHN, C. - Los Alamos Scientific Lab., U. of California, POB 1663, Los Alamos, NM 87545
 GUNDERSEN, M. - Texas Tech. University, Physics, Lubbock, TX 79413
 HAMMOND, Bob - MS 430 E-10 LASL, Los Alamos, New Mexico 87545
 HANES, L. - Physics, North Texas State University, Denton, TX 76203
 HAYES, R. - EE Dept. OT2-32, University of Colorado, Boulder, CO 80307
 HEFLEY, W. - Physics, North Texas State University, Denton, Texas 76203
 HESS, K. - Angewandte Physik der Universität Wien, A-1090, Wien, Austria
 HEHN, J. - Physics, North Texas State University, Denton, TX 76203
 HOLM-KENNEDY, J. - U. of Hawaii, Dept. of Physics and Astronomy, Honolulu, Hawaii 96822
 HAUSER, J.R. - E.E. Dept., North Carolina State U., Box 5275, Raleigh, N.C. 27607
 HEINRICH, H. - Johannes Kepler U., Experimentalphysik II, A-4045, Linz, Auhof, Austria
 HILSUM, C. - Royal Radar Establishment, St. Andrews Road, Great Malvern Worcs WR14 3PS, UK
 HOUSTON, B.B. - Naval Surface Weapons Center, White Oak Lab., Silver Spring, MD 20910
 HUGHES, R.C. - Sandia Laboratoires, Albuquerque, New Mexico 87115
 INOUE, Masataka - Kitanoda 349, Sakai, Osaka, Japan
 IPPEN, E.P. - Bell Laboratories, 4C-418, Holmdel, New Jersey 07733
 JACKSON, R. - Physics, North Texas State University, Denton, Texas 76203
 JANTSCH, W. - Johannes Kepler U., Experimentalphysik A-4045, Linz, Auhof, Austria

- JANI, S.K. - Physics, North Texas State University, Denton, TX 76203
- JACOBONI, C. - Istituto di Fisica, Laboratorio di Elettronica, Via Vivaldi 70, 41100, Modena, Italy
- KAHLERT, H. - Physics, North Texas State University, Denton, TX 76203
- KASPRZAK, L.A. - Mountain Pass Geneva Drive, Hopewell Jct., New York 12533
- KENNEDY, P. - Physics, North Texas State University, Denton, TX 76203
- KIEU, V.C. - Lab. de Physique des Solides, CNRS, 1., Place Aristide Briand, 92190 Meudon, France
- KOBE, D. - Physics, North Texas State University, Denton, Texas 76203
- KOBAYASHI, T. - Dept. of E.E., Kobe University, Rokko, Nada, Kobe 657, JAPAN
- KOLK, M. - Physics, North Texas State University, Denton, Texas 76203
- KROEMER, H. - E.E. & Comp. Sci. Dept., U. of California, Santa Barbara, CA 93106
- KROELL, K. - Gartenstr. 45, 7031 Holzgerlingen, Germany
- KRISHNAN, M. - Physics, North Texas State University, Denton, TX 76203
- LANYON, H.P.D. - Worcester Polytechnic Institute, Worcester, Massachusetts 01609
- LATHAM, P. - Physics, North Texas State University, Denton, TX 76203
- LEHENY, R. - Ball Laboratories, Holmdel, New Jersey 07733
- LEBURTON, J.P. - Inst. de Physique, Université de Liege, Belgium
- LEWINER, C. - GPS Tour 23, Université Paris VII, 2 Place Jussieu, 75005 Paris
- LEITE, R.C.C. - UNICAMP, Campinas, Brazil
- LITTLEJOHN, M.A. - North Carolina State U., 232 Daniels Hall, Raleigh, N.C. 27607
- LIU, M. - Honeywell, 10701 Lyndale Ave. S., Bloomington, Minn. 55420
- LO, Ho W. - Apt. R-6, Jardine Terrace, Manhattan, Kansas 66502
- MAXSON, D. - Physics, North Texas State University, Denton, Texas 76203
- MARSHALL, B.J. - Physics, Texas Tech. U., Lubbock, TX 79406
- MCDANIEL, F.D. - Physics, North Texas State University, Denton, TX 76203
- McAFEE, S.R. - Bell Laboratories, 600 Mountain Ave., Murray Hill, NJ 07974
- McLEAN, F.B. - Harry Diamond Labs., Adelphi, MD 20906
- MEHTA, R. - Physics, North Texas State University, Denton, Texas 76203
- MOSS, S. - Physics, North Texas State University, Denton, Texas 76203
- MEYER, F. - Physics, North Texas State University, Denton, TX 76203
- MOORE, B. - Physics, North Texas State University, Denton, TX 76203
- MUELLER, W. - Inst. f. Physikalische Elektronik, T.U. Wien, A-1040 Wien, Austria
- NAHORY, R. - Bell Laboratories, Holmdel, New Jersey 07733
- NAG, B.R. - Inst. of Radiophysics and Electronics, 92, Acharya Prafulla Chandra Road, Calcutta, 700 009, India
- NOUGIER, J.P. - Centre d'Etudes d'Electronique des Solides, Université des Sciences et Techniques du Languedoc, 34060 Montpellier, Cedex, FRANCE
- NURMIKKO, A. V. - Division of Engineering, Brown University, Providence, RI 02912
- PEARSALL, T.P. - Laboratoire Central de Recherches, THOMSON/CSF, 91401, Orsay, France
- PICKIN, W.F. - Milán 38-A403, Col. Juárez, México, 6 D.F. México
- PILKUHN, M. - Physikalisches Inst., Stuttgart U., Pfaffenwaldring 57, D-7000, Stuttgart 800, W. Germany
- PILLER, H. - 12467 Sherbrook Ave., Baton Rouge, LA 70815
- PRICE, P. - IBM Watson Research Center, POB 218, Yorktown Heights, New York 10598
- RABSON, T. A. - Engineering Dept, Rice U., POB 1892, Houston, Texas 77001
- REDDING, R.W. - Physics, North Texas State University, Denton, Texas 76203
- REINITZ, K. - Johns-Hopkins U., Applied Physics Lab., Laurel, Md 20810
- RESTORFF, J. - Naval Surface Weapons Center, Silver Springs, Md. 20910
- RICE, R. - Physics, North Texas State University, Denton, TX 76203
- SANGSINGKROW, P. - Physics, North Texas State University, Denton, TX 76203
- SCULLY, M. - U. of Arizona, Optical Sciences Center, Tucson, Arizona 85721
- SEARS, R. - Physics, North Texas State University, Denton, TX 76203
- SEILER, D.G. - Physics, North Texas State University, Denton, TX 76203
- SHAH, J. - Bell Laboratories, Holmdel, New Jersey 07733
- SHANK, C.V. - HO 4E-418, Bell Laboratories, Murray Hill, New Jersey 07974
- SHAW, M.P. - Research Inst. for Eng. Sciences, Wayne State U., Detroit, MI 48202
- SHEN, R. - Texas Instruments, P.O. Box 5936, Dallas, Texas 75222
- SHEPARD, P. - Physics, North Texas State University, Denton, TX 76203

SILVER, R.N. - Los Alamos Scientific Lab., U. of Ca., POB 1663, Los Alamos, NM 87545
SMIRL, A.L. - Physics, North Texas State University, Denton, Tx. 76203
SOLOMON, P.M. - IBM Watson Research Center, POB 218, Yorktown Heights, NY 10598
SPECTOR, H.N. - Physics, Illinois Inst. of Technology, Chicago, Ill. 60616
STEPHENS, A. - Physics, North Texas State University, Denton, TX 76203
STORMER, H.L. - Bell Laboratories, Murray Hill, N.J. 07974
SUZUKI, A. - Physics, University of Manitoba, Winnipeg, Manitoba R3T 2N2, Canada
SWINDLE, D.L. - Physics, North Texas State University, Denton, Tx. 76203
SYBERT, J. - Physics, North Texas State University, Denton, TX 76203
TEOH, H. - State University of New York, College at Old Westbury, Box 210, Old Westbury, New York 11568
THORNBUR, K.K. - 23 Mercier Place, Berkeley Heights, New Jersey 07922
TROUTMAN, R. - IBM Systems Products Div., Dept. G39/Bldg 966-2, Essex Junction, VT 05452
TSUI, D.C. - Bell Laboratories, Murray Hill, N.J. 07974
ULBRICH, R.G. - Institut für Physik, Universität Dortmund, Dortmund, FRG
UMENO, M. - Department of Electronics, Nagoya University, Nagoya 464, Japan
VON KLITZING, K. - Physikalisches Institut der Universität Würzburg, 8700 Würzburg, FRG
WASSEF, W.A. - 1109-77 University Crescent, Winnipeg, Manitoba R3T 3N8, Canada
WEBSTER, W. - 179 Woods Drive, Annapolis, Md. 21401
WEISBUCH, C.C. - Ecole Polytechnique, Laboratoire de Physique de la Matière Condensée, 91128 Palaiseau, France
WITTMAN, H. - U.S. Army Research Office, P.O. Box 12211, Research Triangle Park, NC 27709
YEN, H. 3271 W. Sierra Drive, Westlake Village, CA 91361
YOCOM, T. - Texas Tech. University, Lubbock, TX 79413
YU, Ho. - Varo Semiconductor, Inc. POB 676, 1000 N. Shiloh, Garland 75040
ZEHE, A. - Universidad Autónoma Puebla, Escuela de Ciencias Físicas, Calle 4, Sur 104, Puebla, Mexico
ZUKOTYNSKI, S. - Dept. of E.E., U. of Toronto, Toronto, Ontario M5S 1A4

IX. SUMMARY OF PRINCIPLE ACCOMPLISHMENTS DURING
OCTOBER 1, 1976-SEPTEMBER 30, 1977

Papers Published

1. "Magnetic Field Modulation Technique for the Study of Hot Carrier Oscillatory Magnetoresistance Phenomena", H. Kahlert and D. G. Seiler, Rev. Sci. Instrum. 48, 1017 (1977).

Papers Accepted and To Be Published

2. "CO₂ Laser-Induced Hot Electron Effects in n-InSb", B. T. Moore, D. G. Seiler, and H. Kahlert, to be published in Solid State Electronics, about January 1978.
3. "Electric Field Dependence of the Positions and Amplitudes of Magnetophonon Oscillations in n-InSb at 77K", H. Kahlert, D. G. Seiler, and J. R. Barker, to be published in Solid State Electronics, about January, 1978.
4. "Observation of Magnetophonon Structure in Degenerate n-InSb", H. Kahlert and D. G. Seiler, to be published in Solid State Communications.
5. "The Magnetophonon Effect in a Nonparabolic Band: n-type InSb", H. Kahlert, to be published in the Physical Review.

Talks Given at American Physical Society Meeting - March, 1977 in San Diego (See Vol. 22, #3)

1. "High Resolution Measurements of the Hot-Electron Magnetophonon Effect in n-InSb at 77K", H. Kahlert, D. G. Seiler, and A. E. Stephens.

2. "Laser-Induced Hot Electron Transport Effects in n-InSb at 2K", B. T. Moore, D. G. Seiler, and H. Kahlert.
3. "A Magnetic Field Modulation Technique for the Study of Hot Carrier Oscillatory Magnetoresistance", D. G. Seiler and H. Kahlert.

Talks Given at the International Conference on Hot Electrons in Semiconductors, July 6-8, 1977

4. "Electric-Field Dependence of the Positions and Amplitudes of Magnetophonon Oscillations in n-InSb at 77K", H. Kahlert, D. G. Seiler, and J. R. Barker.
5. "CO₂ Laser-Induced Hot Electron Effects in n-InSb", B. T. Moore, D. G. Seiler, and H. Kahlert.

Patent Activity

The process of applying for a patent through ONR procedures is being followed for the magnetic field modulation technique that was discovered this year.